



LABORATORY AND ON-ROAD TESTING OF EXHAUST EMISSIONS OF TWO MODERN CHINA 5 LIGHT-DUTY GASOLINE VEHICLES

Liuhanzi Yang, Yoann Bernard, Francisco Posada, John German

ACKNOWLEDGMENTS

This work was funded through the generous support of the Pisces Foundation, the Energy Foundation China, and the Rockefeller Brothers Fund. The authors acknowledge internal and external reviewers for their guidance and constructive comments, with special thanks to Michael Walsh; Dagang Tang, Yan Ding, and Hang Yin of the Vehicle Emission Control Center, China Ministry of Ecology and Environment; Sheng Su and Yitu Lai of the Xiamen Environment Protection Vehicle Emission Control Technology Center; Ye Wu of Tsinghua University; Shaojun Zhang of Cornell University; Hui He, Rachel Muncrief, Jan Dornoff, Felipe Rodríguez, Anup Bandivadekar, Ray Minjares, and Zifei Yang of the International Council for Clean Transportation.

International Council on Clean Transportation
1225 I Street NW Suite 900
Washington, DC 20005 USA

communications@theicct.org | www.theicct.org | [@TheICCT](https://twitter.com/TheICCT)

© 2018 International Council on Clean Transportation

TABLE OF CONTENTS

Executive Summary	ii
Abbreviations	1
1 Introduction	2
2 Methodology	4
2.1 Test vehicle selection	4
2.2 Test matrix.....	4
2.3 Laboratory test methodology	5
2.4 RDE test methodology.....	7
3 Results	10
3.1 Results of laboratory test.....	10
3.2 Results of RDE test.....	12
4 Discussion	18
4.1 Discussion of laboratory results	18
4.2 Discussion of RDE results.....	28
5 Conclusions and policy recommendations	31
5.1 Conclusions.....	31
5.2 Policy recommendations.....	32
References	34
Appendix	37

EXECUTIVE SUMMARY

A growing base of studies worldwide has demonstrated that vehicle emissions under real-world driving conditions can be significantly higher than certified emissions values as tested in the laboratory. One of the main reasons is deficiencies in type-approval protocols. The current light duty vehicle (LDV) test cycle in China, the New European Driving Cycle (NEDC), is an unrealistic representation of on-road driving conditions. In response to this problem, as part of China's adoption of more stringent China 6 emissions standard, China is shifting away from the NEDC and adopting a more representative cycle, the Worldwide Harmonized Light Vehicles Test Procedure (WLTP), adding real-driving emissions (RDE) testing requirements, and introducing a comprehensive in-use compliance program. Under the new testing framework, manufacturers will have to demonstrate that vehicles show compliance with emissions limits not only in laboratory tests but also in real-world driving throughout the vehicle's in-use duration as required by regulations.

This paper aims to develop a better understanding of real-world emissions performance of LDVs in China. In this study, two modern China 5 gasoline cars were tested in the laboratory on a chassis dynamometer and on the road by using a Portable Emissions Measurement System (PEMS). The tests were conducted at the Xiamen Environment Protection Vehicle Emission Control Technology Center. Laboratory chassis dynamometer tests included standard China 5 type-approval tests (NEDC, 25°C, and cold start) and tests under various cycles and conditions to reflect real-world complexity, such as low/high ambient temperature, cold/hot start, air conditioning operation, and on the WLTP.¹ The RDE test routes, equipment, and ambient conditions all met the provisions in the China 6 RDE regulation.

Figure ES1 presents an overview of the laboratory and RDE test results for the two vehicles. It should be noted that Vehicle A is classified as a Type 1 vehicle while Vehicle B is a Type 2,² so different emissions limits apply to the two cars. Vehicle A, a 1.6 L small sedan with port fuel injection (PFI), and Vehicle B, a 2.4 L multi-purpose vehicle with gasoline direct injection (GDI), both passed the China 5 type-approval tests over the NEDC. However, nitrogen oxides (NO_x) emissions of Vehicle A on the NEDC after a hot start and on the standard WLTP with a cold start increased significantly and exceeded the China 5 limit. In addition, the NO_x results of Vehicle A in RDE tests were on average 1.6 times the China 5 laboratory limit. NO_x emissions from Vehicle B were even lower than the China 6b limit under all laboratory and RDE tests. Our in-depth investigation indicates that the high NO_x of Vehicle A is most likely attributable to a poor and lenient design of the fuel injection control strategy.

Both vehicles show significantly higher emissions of carbon monoxide (CO) over the more dynamic WLTP tests. This is probably because the engines were running at rich air-to-fuel ratios during the higher engine loads imposed by harder accelerations in the

1 Both the NEDC and the WLTC have testing protocol requirements that specify the test cell temperature at 25°C for the NEDC and 23°C for the WLTC. This testing project covered tests under low (14°C) and high (30°C) temperatures. Hot start tests refer to tests carried out within 50 minutes of finishing an NEDC or WLTC test, when the engine block, coolant, and aftertreatment control systems are well above the temperatures corresponding to cold-start tests.

2 Light-duty vehicle categories in China are based on the EU classification with some deviation:
 Type 1 vehicles: M1 vehicles for no more than six passengers including driver, and GVWR ≤ 2.5 tons.
 Type 2 vehicles: Other light-duty vehicles (including N₁ light commercial vehicles) further divided into three classes based on the reference mass.

WLTP. In RDE tests, CO emissions in some cases exceeded the China 5 limit by 2.8 times. The results provide sound arguments that CO emissions from gasoline cars are not properly controlled under real-world driving conditions and need particular attention from the regulators.

Particle number (PN) emissions from Vehicle A, a conventional PFI car, managed to stay at low levels in all circumstances, while Vehicle B, a GDI car, had an order of magnitude higher PN emissions in laboratory and RDE tests compared with Vehicle A. Our results highlight the importance of better controlling particle emissions from GDI cars.

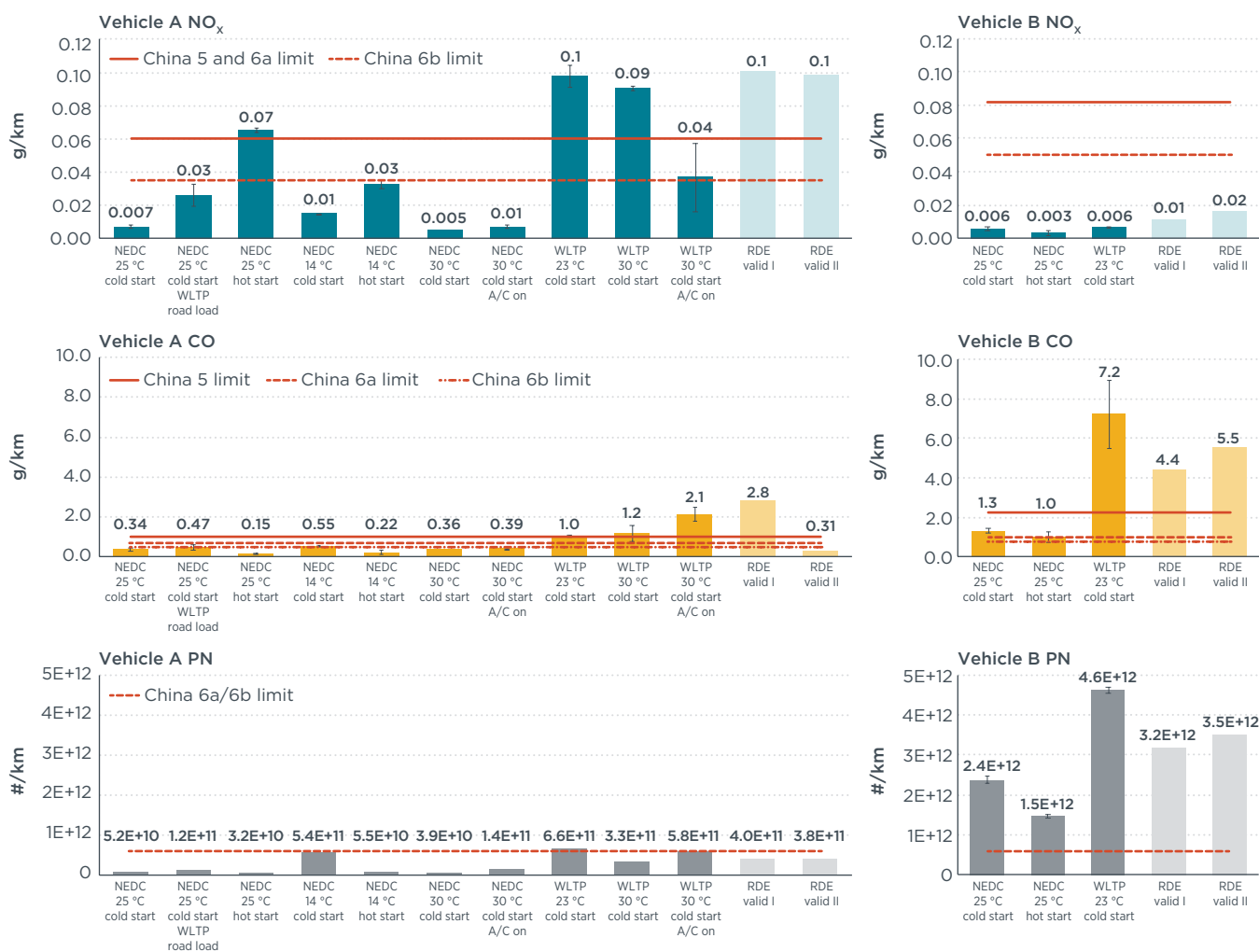


Figure ES 1 An overview of laboratory and RDE test results of two China 5 gasoline cars. Vehicle A is a small car with port fuel injection (PFI); Vehicle B is a multi-purpose vehicle with gasoline direct injection (GDI). Error bars indicate standard deviation.

This testing project includes the first third-party-run RDE testing program in China and provides a good basis for further study of real-world emissions from LDVs. The findings from this study point to several policy implications related to future emissions standards and in-use compliance programs in China. Specific recommendations include:

- » The new China 6 LDV standard, which will take effect July 1, 2020, is a significant step toward effectively controlling real-world emissions from LDVs in China. We

recommend that provinces and cities facing severe air pollution implement the China 6 standard as early as possible.

- » The China 6 RDE regulation does not include cold-start operation in the data evaluation process. This study demonstrated again that cold start is an important contributor to vehicle emissions. The inclusion of cold starts in the RDE requirements will be essential for ensuring the use of optimum emissions control technologies and controlling real-world emissions. We recommend further studies on the impacts of cold starts in future RDE testing programs and inclusion of cold starts in the RDE regulation as soon as possible.
- » CO emissions will be monitored in RDE tests, but no CO limits have been set in the China 6 regulation. Results in this study suggest that CO from gasoline cars can be substantial under real-world driving conditions. As total hydrocarbons (THC) and CO emissions tend to rise and fall together, limiting CO emissions would indirectly limit THC emissions from gasoline cars. This includes toxic species such as benzene, toluene, ethylbenzene, and xylene, and contributes to secondary organic aerosols, an important component of ambient $PM_{2.5}$, in the atmosphere.
- » The results add to growing evidence that PN emissions from GDI vehicles are significant. Further investigation on particle size distribution would be important to better understand the PN emissions characteristics of GDI vehicles.
- » On-road PEMS testing is an excellent tool for in-use compliance programs. Enhanced laboratory testing can serve as a pre-screening tool to help identify high emitters and defeat devices, which are equipment designed to interfere with or disable emissions control systems.

ABBREVIATIONS

A/C	Air Conditioning
CF	Conformity Factor
CO	Carbon monoxide
CO ₂	Carbon dioxide
EF	Emissions Factor
GDI	Gasoline Direct Injection
LDV	Light-duty vehicle
MEE	Ministry of Ecology and Environment of China
MEP	Ministry of Environmental Protection of China
NEDC	New European Driving Cycle
NO _x	Nitrogen oxides
OBD	On Board Diagnostics
PEMS	Portable Emissions Measurement System
PM	Particle mass
PN	Particle number
PFI	Port Fuel Injection
RDE	Real-Driving Emissions
RPA	Relative Positive Acceleration
THC	Total Hydrocarbons
TWC	Three-way catalyst
v*a	Velocity times acceleration
WLTC	Worldwide Harmonized Light Vehicles Test Cycle
WLTP	Worldwide Harmonized Light Vehicles Test Procedure

1 INTRODUCTION

It has been widely recognized that real-world vehicle emissions can be substantially higher than the values certified on chassis dynamometer tests in a laboratory. In the United States and Europe, some serious concerns have emerged in the past few years over the real-world emissions performance of diesel cars. Studies of comprehensive remote sensing and on-road PEMS measurement indicate that NO_x emissions from diesel cars have not decreased in line with the limits set by the standards (Carlaw, Beevers, Tate, Westmoreland, and Williams, 2011; Carlaw and Rhys-Tyler, 2013; Franco, Posada Sánchez, German, and Mock, 2014). NO_x emissions from some modern diesel cars exceeded the limit by a factor of more than 25 in real-world driving, with average NO_x emissions factors of seven times the limit (Franco et al., 2014).

In China, nearly 97% of LDVs are powered by gasoline. The ICCT's China PEMS meta-study (Yang, 2018) found that emissions standards have played an important role in reducing vehicle emissions from LDVs in China. Real-world NO_x, CO, and THC emissions from gasoline cars have declined significantly as vehicle technology has improved from China 0 to China 4/5. However, some modern China 4 and China 5 gasoline cars were found to have significantly high NO_x and CO emissions during real-world driving.

One of the major reasons behind the real-world emissions disparity is that current type-approval procedures, including driving cycle and test procedures, cannot capture the whole range of the real-world vehicle operating conditions (Kågeson, 1998; Mellios, Hausberger, Keller, Samaras, and Ntziachristos, 2011; Kadijk and Ligterink, 2012; Kadijk et al., 2012). In response, the European Union has replaced the NEDC test procedure with the WLTP and introduced RDE testing, taking effect in September 2017 (European Commission, 2016a, 2016b). The WLTP includes not only a test cycle that is more representative of real-world driving but also more robust provisions on road load and test weight determination. With the new RDE provisions, LDVs have to pass not only the chassis dynamometer test in the laboratory but also a PEMS test in real-world driving conditions.

Emissions regulations in China largely follow EU regulatory precedent, with the implementation dates of the China LDV standards generally lagging behind the equivalent EU standard by five to eight years. In December 2016, the China Ministry of Environmental Protection (MEP)³ released the final rule of the China 6 LDV emissions standard (MEP, 2016a). The new China 6 standard also shifts from the NEDC to the WLTP in the China 6a stage and adopts RDE testing requirements for both type test and in-use compliance test in the China 6b stage. All new vehicles must comply with the RDE provisions starting July 1, 2023. However, the China 6 final rule sets a relatively lenient conformity factor (CF) of 2.1 for NO_x and PN and excludes cold-start emissions from data evaluation. It is yet to be studied whether these requirements are sufficient to address the emissions issues under the full range of operating conditions in real-world driving. In addition, it will be useful to understand how current and emerging emissions control strategies perform under various testing conditions that increasingly reflect real-world driving.

³ In March 2018, MEP was replaced by a new Ministry of Ecology and Environment (MEE). The new ministry is in charge of all responsibilities of the former MEP, responsibilities on climate change under the National Development and Reform Commission, and marine pollution control, underground water pollution regulation, and agricultural pollution control under six other ministries.

LDVs with gasoline direct injection (GDI) have been commercial since the late 1990s and are increasingly emerging on the market worldwide (Queiroz and Tomanik, 1997). Compared with port fuel injection (PFI) autos, GDI cars can offer greater power output, improved fuel consumption efficiency, and performance benefits (Fraser, Blaxill, Lumsden, and Bassett, 2009; Storey et al., 2014). One drawback of GDI technology is that particulate matter emissions from GDI cars are higher than those from conventional PFI vehicles because of different injection methods and operation modes (Hall and Dickens, 1999; Fu, Wang, Li, and Shuai., 2014). Previous research found that particle emissions, especially particle number (PN) from first-generation GDI cars, were significantly higher than from conventional PFI gasoline cars as well as diesel cars with diesel particulate filters (Hall and Dickens, 1999; Khalek, Bougher, and Jetter, 2010; Zhang and McMahon, 2012; Badshah, Kittelson, and Northrop, 2016). In addition, GDI engines can produce a significant amount of ultrafine particles, which might be more harmful to human health than bigger particles (Oberdörster et al. 2004). During a WLTP test, the number of sub-23 nm particles were on average 30%-40% of the total particle number for GDI engines (Giechaskiel and Martini, 2014). Nevertheless, the sub-23 nm particles are not accounted for in the current test protocol in China and the European Union.

To control particle emissions from the growing number of GDI vehicles, the United States has introduced a stringent emissions limit for particle mass (PM). The European Union has tightened PM emission limits as well and has also introduced PN limits for GDI vehicles under the Euro 6 standard. Similarly to the European Union, China has introduced PN limits for GDI cars in the new China 6 standard. Driven by the more stringent Phase 4 fuel consumption standard for LDVs, manufacturers in the Chinese market are increasingly adopting GDI technology. From 2010 to 2015, the market share of GDI-equipped new gasoline passenger cars in China grew from 6% to 29% (Xiao, Yang, and Isenstadt, 2018). In Europe, GDI technology was adopted for more than 43% of all new gasoline vehicles sold in 2016 (the ICCT, 2017). It will be useful to understand the particle emissions behavior of GDI vehicles in the Chinese market.

In summary, the primary objective of this paper is to understand real-world emissions performance of modern gasoline LDVs in China and therefore to support the development of solutions for more realistic vehicle testing procedures and in-use compliance programs in the next phases of emissions standards for LDVs. A second objective is to investigate real-world PN emissions from the current generation of GDI technologies in the Chinese market. A third objective is to gain an understanding of how emissions under varying chassis laboratory testing conditions deviate from those in type-approval testing.

To this end, we employed two modern China 5 gasoline cars, one with PFI and the other with GDI, and performed a comprehensive testing program including laboratory chassis dynamometer tests and on-road PEMS tests.

This remainder of this report is organized as follows: Section 2 describes the vehicle selection, test items, and test methodology applied in this study. Section 3 gives an overview of the test results for both laboratory and RDE tests. Section 4 presents detailed analysis and discussion of the implications of the test results. Section 5 concludes with a summary of key findings and policy recommendations.

2 METHODOLOGY

2.1 TEST VEHICLE SELECTION

Two China 5 gasoline cars were tested in this project. Table 1 presents an overview of the specifications of the two vehicles. Both vehicles were rented from a car rental company. Vehicle A is a PFI car and Vehicle B is a GDI car. Vehicle A is classified as a Type 1 vehicle while Vehicle B is a Type 2,⁴ so different emissions limits apply to the two cars. Both vehicles are equipped with three-way catalyst (TWC) for controlling exhaust emissions. Neither car has a gasoline particulate filter.

Table 1 Test vehicles specifications

	Vehicle A	Vehicle B
Applicable emission standard	China 5	China 5
Model year	2016	2016
Fuel injection	PFI	GDI
Mileage at test start/km	1,290	7,262
Curb weight/kg	1,265	1,860
Max. weight/kg	1,775	2,470
Test Fuel	China 5 reference gasoline	China 5 reference gasoline
Engine displacement/L	1.6	2.4
Engine aspiration	Natural	Natural
Max. engine power/kW	81	137
Max. engine torque/Nm	155	240
Emissions after-treatment	TWC	TWC
Drive train	Front wheel drive	Front wheel drive
Transmission	6-Automatic Transmission	6-Automatic Transmission
Type-approval fuel consumption L/100km	6.9	10.0

The sample vehicles were carefully inspected before testing. The main inspections included vehicle condition, configuration of key emissions control components, maintenance records, and on-board diagnostics (OBD) check. The powertrain, the intake and exhaust system, and the canister purge system were checked to ensure they were functioning well. All key components of the two cars complied with type-approval declarations. Maintenance records showed that the sample vehicles were well maintained as required by the operation manuals. There were no online or permanent fault codes in OBD checks. The same batch of China 5 reference gasoline was used for testing.

2.2 TEST MATRIX

The testing campaign included chassis dynamometer testing in a laboratory and on-road testing using PEMS equipment. The test matrix is listed in Table 2. Test No. 1 was

⁴ Light-duty vehicle categories in China are based on the EU classification with some deviation:
 Type 1 vehicles: M1 vehicles for no more than six passengers including driver, and GVWR \leq 2.5 tons.
 Type 2 vehicles: Other light-duty vehicles (including N₁ light commercial vehicles) further divided into three classes based on the reference mass.

a standard NEDC type-approval test. Tests No. 2 to No.10 were enhanced laboratory tests—we changed the test conditions and procedures, aiming at quantitatively identifying the impacts of road load determination⁵, cold start, ambient temperature, air conditioning operation, and WLTP test procedure. Test 11 was a China 6 RDE test. The test route, trip dynamics conditions and trip normality all met the China 6 RDE requirements. For Vehicle A, all 10 laboratory test items were conducted. For Vehicle B, only Tests No. 1, No. 3 and No. 8 were performed in the laboratory because of funding limitation. Except for Test No. 5, two repeated tests were conducted to reduce uncertainty of the results.

Table 2 Test matrix

Test No.	Test type	Start	Ambient temperature	A/C	Road load	Number of tests for Vehicle A	Number of tests for Vehicle B
1	NEDC	Cold	25°C	Off	NEDC	2	2
2	NEDC	Cold	25°C	Off	WLTP	2	0
3	NEDC	Hot	25°C	Off	NEDC	2	2
4	NEDC	Cold	14°C	Off	NEDC	2	0
5	NEDC	Hot	14°C	Off	NEDC	1	0
6	NEDC	Cold	30°C	Off	NEDC	2	0
7	NEDC	Cold	30°C	On	NEDC	2	0
8	WLTP	Cold	23°C	Off	WLTP	2	2
9	WLTP	Cold	30°C	Off	WLTP	2	0
10	WLTP	Cold	30°C	On	WLTP	2	0
11	RDE test (22°C-28°C)					3	3

*Note: WLTP road load was calculated according to China 6 standard.
The hot-start tests were performed 50 minutes after conducting NEDC precondition.
Test No. 5 was conducted only once because of funding limitation.
RDE tests include an invalid RDE test for each vehicle.*

2.3 LABORATORY TEST METHODOLOGY

Test equipment

All tests were conducted by Xiamen Environment Protection Vehicle Emission Control Technology Center (VETC, see Figure 1). This laboratory is equipped with Imtech climatic chamber, AVL 4WD chassis dynamometer, AVL i60 series exhaust sampling and analysis system, and TSI particles counting system. The specifications of the equipment are provided in the Appendix. The equipment was calibrated and checked according to VETC's quality assurance system, which is stricter than the China 5 requirements.



Figure 1 LDV emissions test lab of VETC

⁵ The WLTP road load determination includes more accurate determination of the vehicle's aerodynamic drag and rolling resistance, as well as a revised method of determining vehicle mass for test purposes that increases the mass used for testing.

The ambient temperature and humidity were set by the climatic chamber. Silicon pipe was used to connect exhaust pipe and Constant Volume Sampler (CVS) system. The system sampled and analyzed the gaseous emissions both online and by bag. The particulate system sampled the particulate matter on the filters, and the filters were weighted according to legislation requirements. The PN system counted the diluted PN. Engine specific parameters were recorded through the vehicles' OBD ports using a commercially available Controller Area Network (CAN) logging software called DiagRA® D from RA Consulting GmbH. OBD parameters included engine speed, engine load, and exhaust temperatures.

Road load determination

Two methods for determination of vehicle road load were used in this project. The NEDC road load was declared by the vehicle manufacturers in the type-approval procedure. The VETC lab didn't have the capacity to conduct vehicle coast-down tests, so the WLTP road load was calculated using the equations by vehicle frontal area and curb weight in the China 6 standard, which is identical to the WLTP regulation. Figure 2 illustrates the road load difference between two methods for Vehicles A and B.

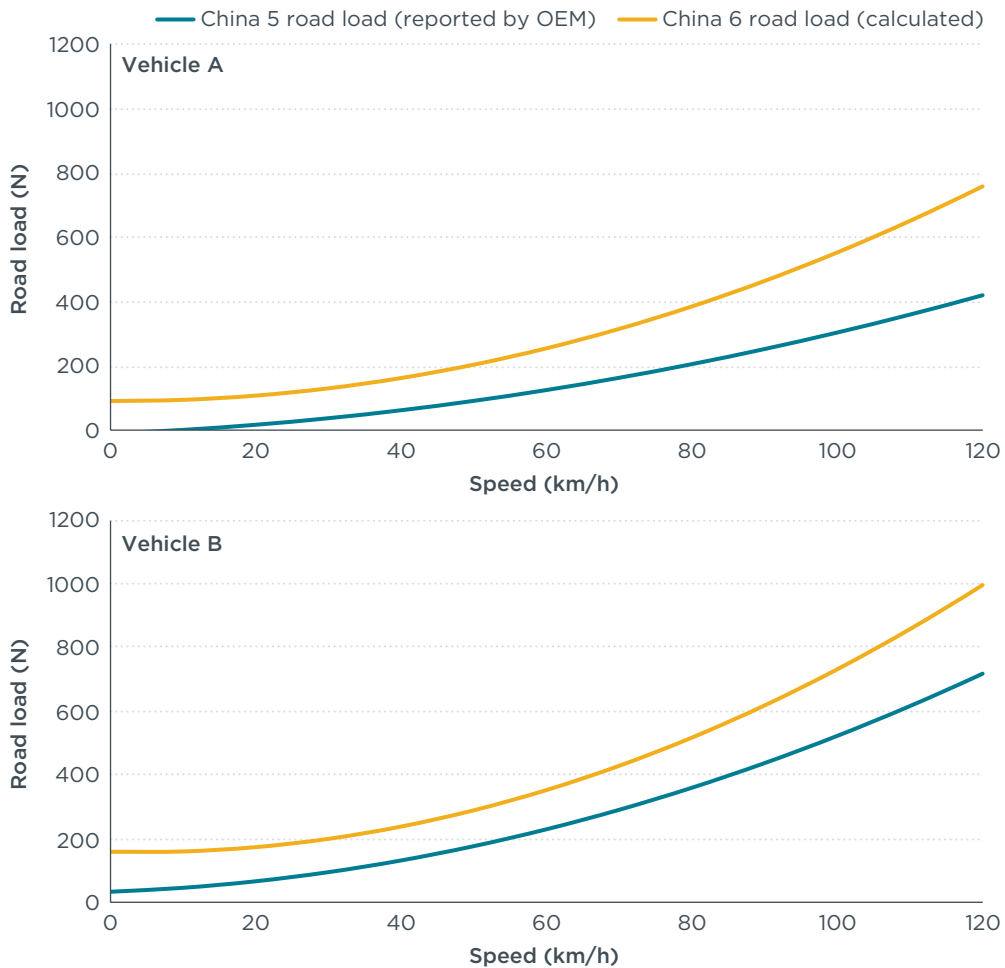


Figure 2 Road load setting for Vehicles A and B using two methods

Air conditioning testing

The air conditioning (A/C) test was conducted only on Vehicle A. The ambient temperature was set at 30°C. The A/C was turned on after engine ignition. Then, the A/C was switched to full cold and recirculation mode, the flowrate of the fan was switched to half, and the windows were closed during the whole test.

2.4 RDE TEST METHODOLOGY

Test equipment

The AVL Concerto M.O.V.E. PEMS system was employed for the RDE tests. The specifications are listed in Table A2 in the Appendix. The system configurations are shown in Figure 3. Second-by-second CO, carbon dioxide (CO₂), NO, NO₂, O₂, and PN emissions were measured and recorded. THC and PM emissions were not measured in the RDE tests.

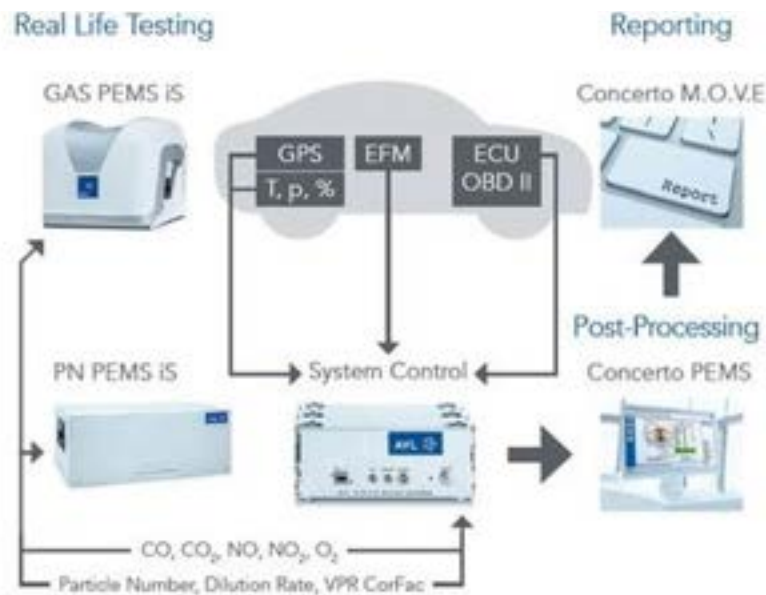


Figure 3 AVL Concerto M.O.V.E system configuration

RDE test routes

The RDE test route was selected in Xiamen according to the requirements in the China 6 standard. Figure 4 shows the map of the testing route. It consists of three parts, urban, rural, and motorway. The overall distance was about 80 km and the altitude was lower than 100 m. The route meets all the provisions of the China 6 regulation.



Figure 4 RDE test route (the blue point is the starting point)

RDE test procedures

The PEMS was installed in the trunk of the sample vehicle. A silicon pipe was used to connect the exhaust pipe to the Pitot tube flowmeter. To reduce the impact of vibration, the GAS-PEMS and PN-PEMS devices were fastened by secure belts. Four fully charged lithium batteries were connected to power the PEMS during the RDE test. Figure 5 shows the PEMS installation of a sample vehicle. A driver and one technician sat in the car for each test. As cold start is excluded in the China 6 RDE regulation, the emissions data during cold start was not recorded in this program.



Figure 5 PEMS installation

Verification tests between PEMS and CVS on chassis dynamometer

To ensure test accuracy, verification tests were carried out between PEMS and CVS (see Figure 6). In the laboratory, vehicle emissions were tested by the PEMS and CVS systems at the same time. As showed in Table 3, the relative deviations between two systems were within the China 6 regulated limits for all tests.



Figure 6 PEMS verification on chassis dynamometer

Table 3 PEMS Verification test results

Vehicle	Test	Equipment	CO (g/km)	NO _x (g/km)	CO ₂ (g/km)	PN (#/km)
Vehicle A	WLTP 23°C cold start	CVS	0.921	0.102	189	4.27E+11
		AVL MOVE	0.809	0.101	195	4.41E+11
		Relative deviation	-12%	-1%	3%	3%
Vehicle A	WLTP 23°C cold start	CVS	0.724	0.114	190	3.93E+11
		AVL MOVE	0.692	0.125	201	4.09E+11
		Relative deviation	-4%	9%	6%	4%
Vehicle B	WLTP 23°C cold start	CVS	7.23	0.00800	271	4.16E+12
		AVL MOVE	6.82	0.00683	286	5.58E+12
		Relative deviation	-6%	-15%	6%	34%
Relative deviation limit in China 6			±15%	±15%	±10%	±50%

Data analysis method

The final emissions factors of the RDE tests were calculated using the moving average window method according to the China 6 RDE regulation.

3 RESULTS

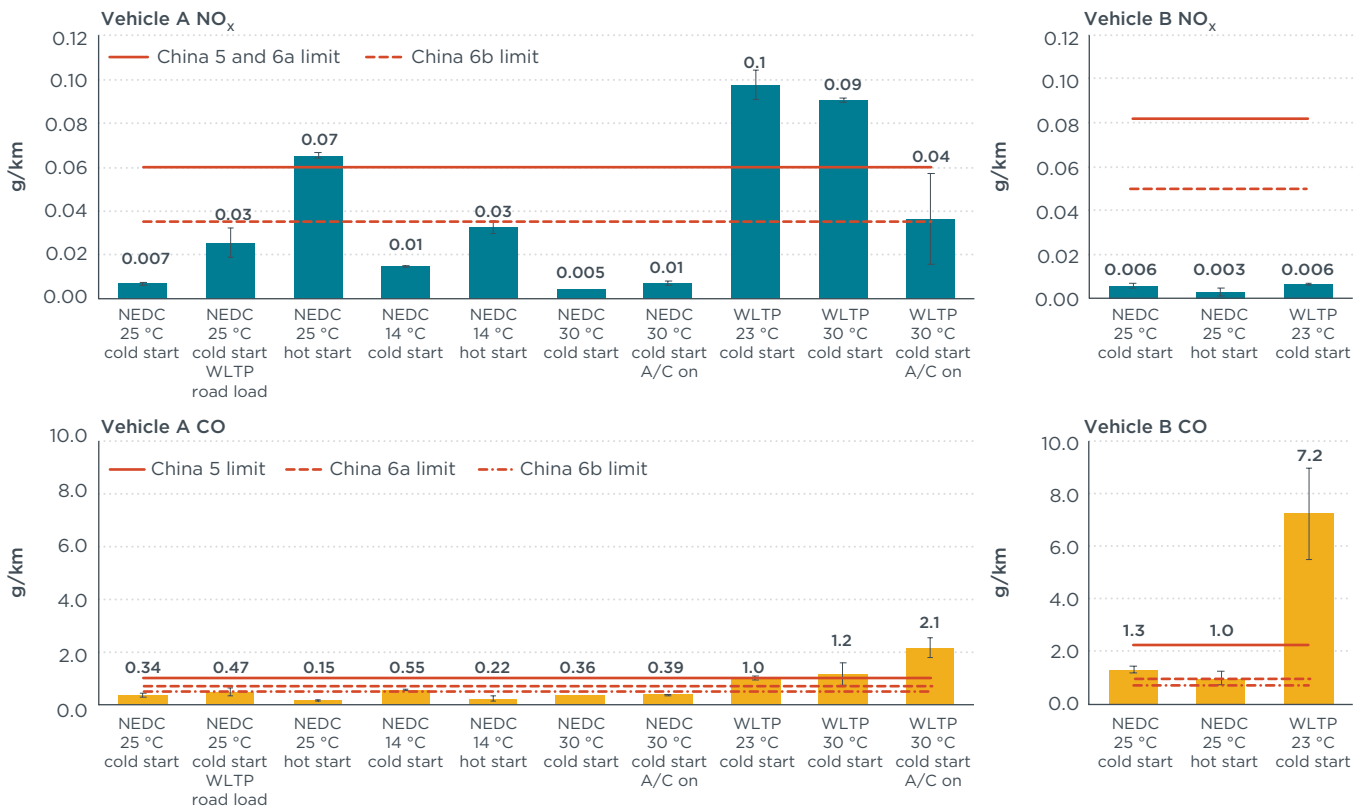
In this section, we present an overview of the laboratory and RDE test results. It should be noted that Vehicle A is a small sedan with curb mass of 1,265 kg, and Vehicle B is a multi-purpose vehicle with curb mass of 1,860 kg, so different emissions limits apply to the two vehicles.

3.1 RESULTS OF LABORATORY TEST

Figure 7 presents a summary of the laboratory test results for the two vehicles. Both vehicles passed the China 5 regulatory test (NEDC 25°C cold start) for all pollutants.

The impact of hot starts and their influence on emissions were studied in both vehicles. The NO_x emissions factor (EF) of Vehicle A over the NEDC 25°C hot start was 10 times more than the EF over the NEDC 25°C cold start. Similar results can be found at 14°C. The result is surprising because it is widely known that vehicle emissions can be easily reduced once the engine and its after-treatment are warmed up. For Vehicle B, the NO_x EF over the NEDC hot start was half of that over the NEDC cold start, which is the expected result.

Road load settings and test cycle also had a huge influence on NO_x emissions for Vehicle A. The NO_x EF over the NEDC 25°C using calculated WLTP road load parameters of Vehicle A was three times higher than the result when using the manufacturer’s declared road load settings for type approval. The NO_x results for Vehicle A over the standard WLTP was 13 times higher than over the standard NEDC, 50 percent above the China 5 standard and more than twice the China 6 standard. However, this was not the case for Vehicle B. The NO_x EF over the WLTP of Vehicle B was at the same level as over NEDC, one-13th of the China 5 and 6a limit. To better understand these consistent results, an in-depth analysis on instantaneous emissions rates and engine signals is provided in the next section.



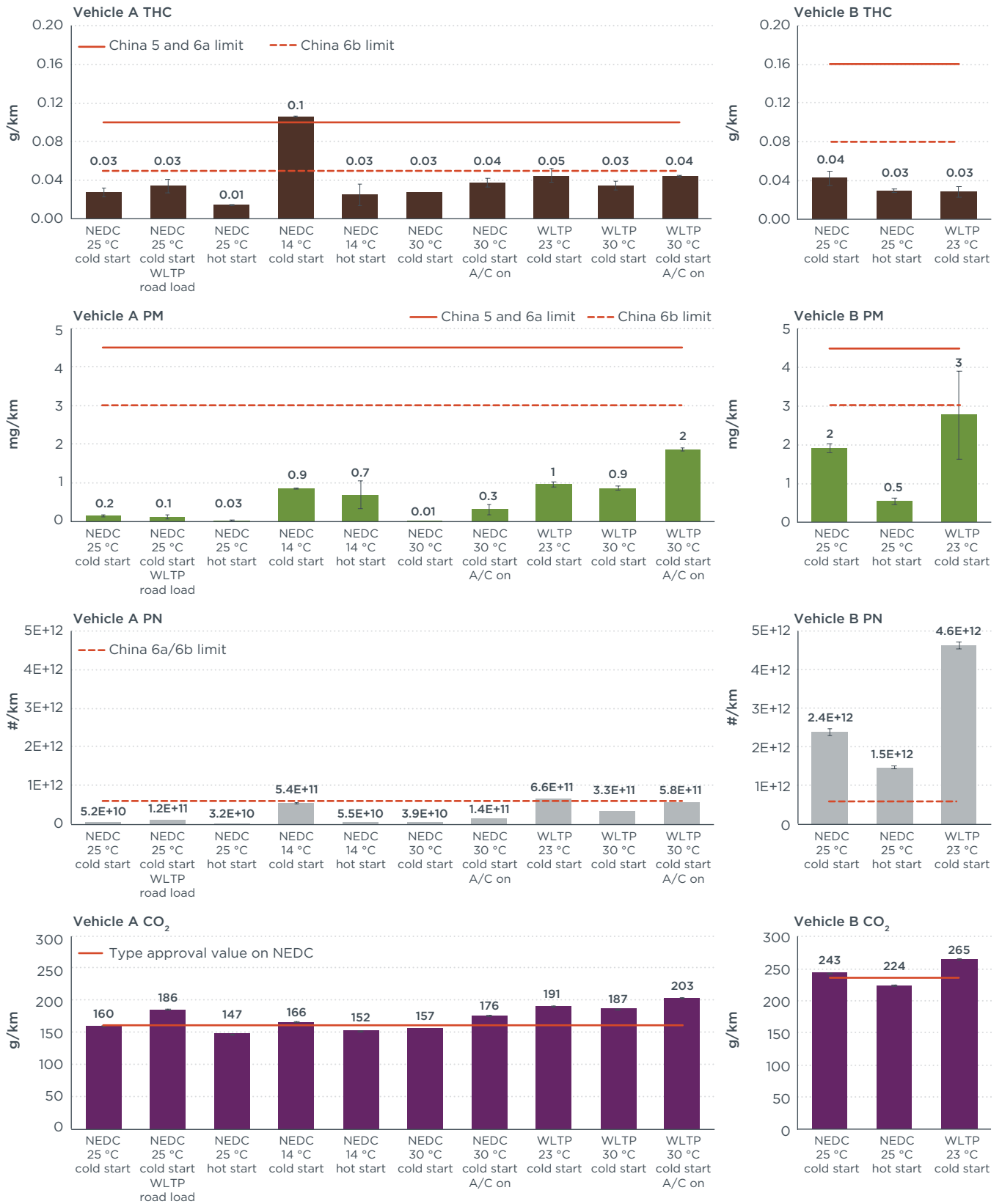


Figure 7 Overview of laboratory NO_x, CO, THC, PM, PN, and CO₂ emissions factors under different laboratory tests (error bars indicate standard deviation)

For CO emissions, both vehicles held below the China 5 limit over all NEDC tests. However, the CO EFs of both vehicles elevated significantly over the WLTP tests. The CO EFs of Vehicle A over the WLTP 23°C, 30°C, and 30°C with A/C on were 1.0 time, 1.2 times, and 2.1 times the China 5 limit. The CO EF of Vehicle B over the WLTP 23°C was 3.4 times the China 5 limit. Engine-out CO is almost always related to fuel enrichment strategies – the richer the air-to-fuel ratio compared with the ideal proportion, the higher the CO output due to incomplete combustion. In addition, CO oxidation in the catalyst is not effective at richer air-to-fuel ratios, leading to orders of magnitude increases in CO. The higher CO emissions on the WLTP thus indicate that both vehicles spent a significant amount of time in enrichment, compared with the NEDC. The WLTP includes higher acceleration rates and more transient operation than the NEDC, for which it appears these vehicles were not calibrated properly to maintain emissions control.

The THC emissions from both vehicles stayed below the China 5 limit for all test conditions, except for the test over the NEDC at 14°C cold start, probably due to the colder ambient temperature increasing the time before catalyst light-off. This shows that tailpipe THC emissions are properly controlled with TWC for modern gasoline cars.

For PM emissions, both vehicles passed the China 5 standard under all test conditions. It can be observed that cold starts, ambient temperature, and driving style are the major factors that influence PM emissions from gasoline cars. For Vehicle A, the PM EF over the NEDC 14°C cold start was 4.5 times the result over the NEDC 25°C, and the PM EFs over the WLTP tests were four to eight times higher than the type-approval value over the NEDC. For Vehicle B, the PM EF over the standard NEDC cold start was four times the finding over a hot start, and the PM EF over the standard WLTP was 50% higher than the value over the standard NEDC test.

For PN emissions, the current China 5 standard doesn't include any PN limits for gasoline cars. In Figure 7, we plot the PN limit of the new China 6 standard as a reference. Vehicle A, a PFI car, passed the China 6 PN limit under all test conditions, except over the WLTP 23°C cold start. However, the PN EFs from Vehicle B, a GDI car, exceeded the China 6 limit over all tests. The PN EFs of Vehicle B over the standard NEDC, NEDC hot start, and standard WLTP were four times, two times, and eight times the China 6 limit. The results added to growing evidence that PN emissions from currently calibrated GDI cars are significantly high and should receive special attention from regulators.

In Section 4.1, we perform an in-depth analysis to identify the impacts of cold starts, driving cycles, ambient temperature, and A/C operation on exhaust emissions.

3.2 RESULTS OF RDE TEST

The RDE test is conducted on public roads open to traffic, so it covers a broader range of driving conditions than a laboratory test. For regulatory purposes, there are some boundary conditions that have been set in the regulation to verify the validation of an RDE trip. Specific provisions include total trip duration, minimum distance for each segment (urban, rural, motorway), ambient temperature, altitude, trip dynamic requirements, etc. The objective of setting trip dynamic requirements is to exclude driving conditions that are considered too aggressive or too mild.

In this section, we firstly conduct a verification of trip dynamics for each RDE trip. Then, an overview of the final test results based on regulatory data process method, the moving average window method, is presented.

3.2.1 Verification of trip dynamics

In the China 6 and the EU RDE regulation, relative positive acceleration (RPA) and the 95th percentile of the product of vehicle speed and positive acceleration ($v \cdot a_{\text{pos}[95]}$) are used to determine the overall excess or absence of dynamics, or the aggressiveness or mildness, of a trip.⁶ The 95th percentile of $v \cdot a_{\text{pos}}$ is used to determine the upper limit, and RPA is used for the lower limit. To be valid, the $v \cdot a_{\text{pos}[95]}$ and RPA of the urban, rural, and motorway segments of an RDE trip must be below the $v \cdot a_{\text{pos}[95]}$ upper limit and above the RPA lower limit. Figure 8 presents the trip dynamics results for three RDE trips of each vehicle. For both vehicles, the RPA of urban driving of the first RDE trips were below the lower limit of the dynamic boundary condition. This suggests that RDE Trip 1 of both vehicles was too passive and should be considered invalid. The dynamics of Trip 2 and Trip 3 of both vehicles fell inside the dynamic boundary conditions, so they were considered valid.

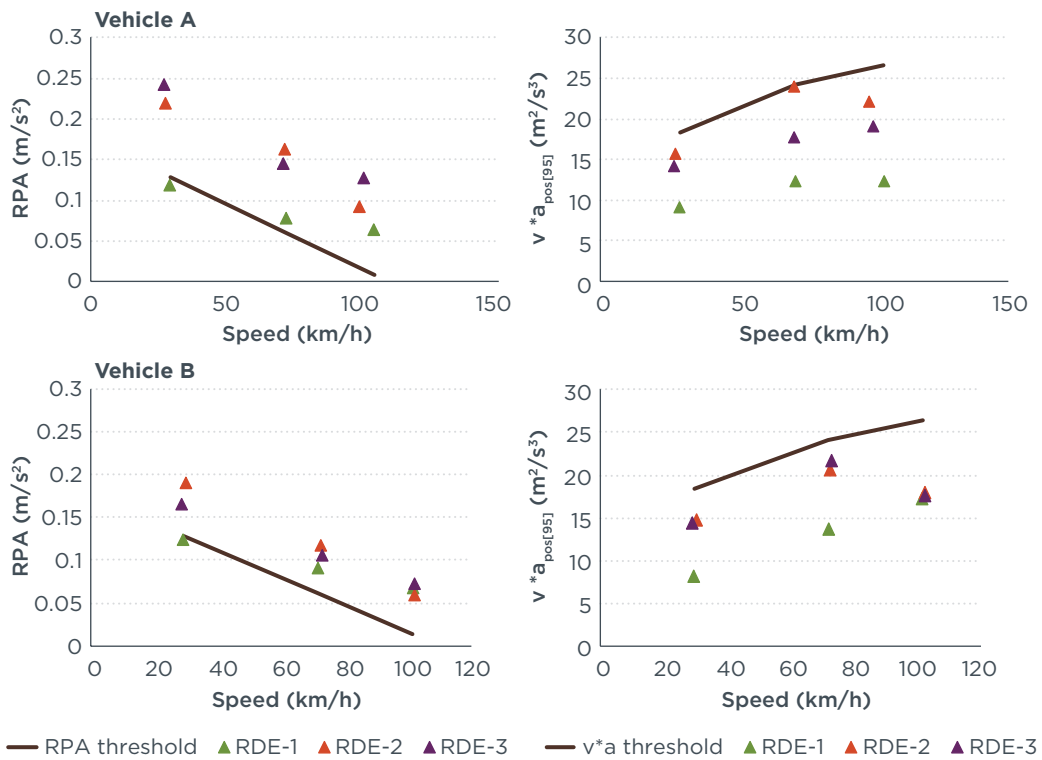


Figure 8 Trip dynamics of three RDE trips for Vehicles A and B

In the following discussion, RDE Trip 1 is marked as RDE-mild. RDE Trip 2 and Trip 3 are marked as RDE valid-I and RDE valid-II.

Figure 9 presents a comparison of instantaneous driving points of a valid RDE test, WLTP and NEDC. The figure clearly indicates that the NEDC is a mild driving cycle with primarily steady-state speed operation and, thus, does not realistically represent real-world driving conditions. The WLTP covers a wider range than the NEDC and adds speed transients but is still relatively mild. The RDE covers the widest range of operation

⁶ RPA is defined as the integral of vehicle speed multiplied with the time interval and the positive acceleration, divided by the total distance of each speed segment. $v \cdot a_{\text{pos}[95]}$ is defined as the 95th percentile of the instantaneous vehicle speed multiplied with the positive acceleration above 0.1 m/s².

points and better represents actual on-road driving behaviors, although the cap on $v \cdot a_{\text{pos}[95]}$ still excludes more aggressive driving with the largest emissions impacts.

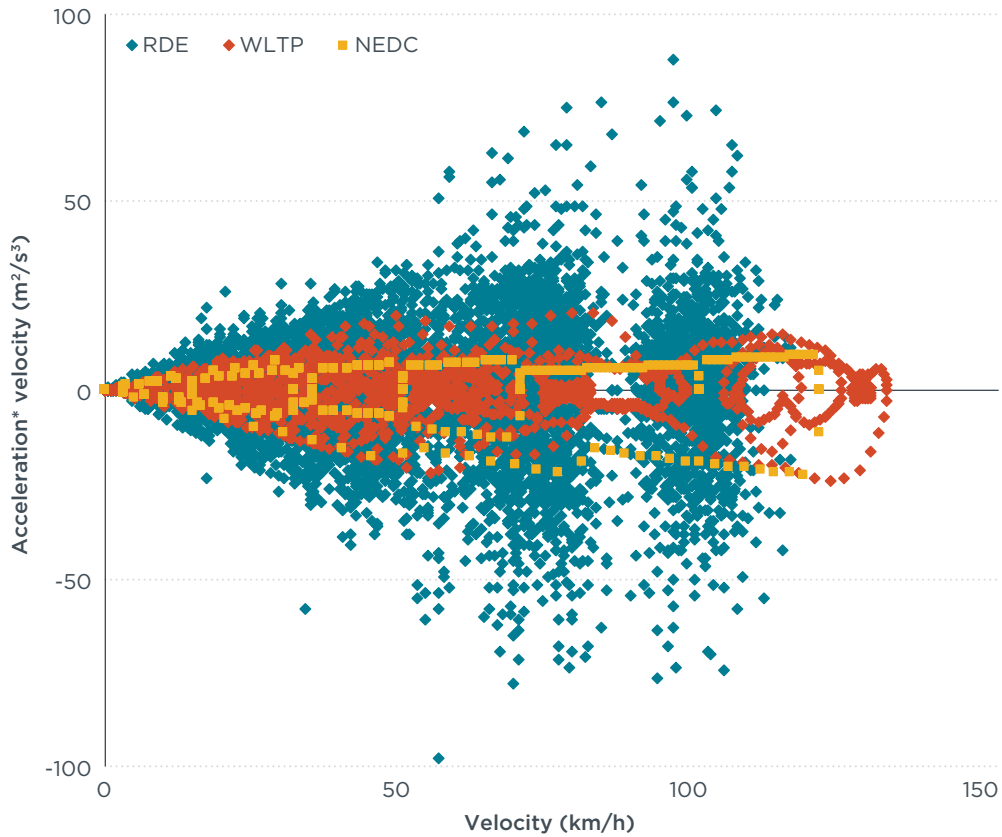


Figure 9 Instantaneous velocity and $v \cdot a$ of valid RDE, WLTP and NEDC trips

3.2.2 Results by moving average window method

For RDE data processing, the moving average window method developed by the European Commission Joint Research Center is adopted in the China 6 RDE regulation. In this study, the second-by-second data collected in an RDE trip were processed by AVL software called Concert using the moving average window method. Table 4 provides an overview of the final CFs of both vehicles. The CFs of CO and NO_x were calculated as the ratio of real-world EFs to the China 5 laboratory emissions limits. For PN, no limits are set for gasoline cars in the China 5 standard. Therefore, the China 6 PN limit was used as a reference. The CFs of CO₂ were calculated as the ratio of on-road CO₂ EFs to the type-approval values over the NEDC published by the Ministry of Industry and Information Technology.

It should be noted that cold starts were excluded in the data processing method under the China 6 regulation. Because there are no regulatory RDE test requirements in the China 5 standard, China 6 RDE limits are presented in Table 4 as a reference.

Table 4 Conformity factors of criteria pollutants and CO₂ emissions of three RDE tests for Vehicles A and B

Vehicle No.	Test No.	Conformity factor			
		CO ₂	CO	NO _x	PN
China 6 limit		N.A.	N.A.	2.1	2.1
Vehicle A (PFI)	RDE mild	0.9	0.03	0.3	0.1
	RDE valid-I	1.6	2.8	1.7	0.7
	RDE valid-II	1.5	0.3	1.7	0.6
Vehicle B (GDI)	RDE mild	1.0	0.5	0.1	3.9
	RDE valid-I	1.5	1.9	0.1	5.3
	RDE valid-II	1.5	2.4	0.2	5.8

For the RDE-mild trips of both vehicles, the overall on-road CO₂ emissions were equal to or less than type-approval values over the NEDC, indicating that both trips were too mild to reflect real-world driving conditions. For the valid trips, the average CO₂ emissions of Vehicles A and B are around 50% higher than type-approval test results. For Vehicle A, the CO CF of RDE valid-I was 2.8 times the laboratory limit. This could be attributed to the fact that the driving style of this trip was too aggressive—the $v^*_{a_{pos[95]}}$ of this trip approached the upper limit of dynamic boundary conditions (see Figure 8). The average NO_x EF of valid RDE trips for Vehicle A was 1.7 times the China 5 laboratory limits, and the PN CF was 35% lower than the laboratory limit, indicating that Vehicle A may pass the RDE test if RDE requirements apply to China 5 LDVs. For Vehicle B, the CO EF of valid RDE trips was on average 2.15 times the China 5 laboratory limit. The average NO_x CF of valid RDE trips of Vehicle B was 85% lower than the China 5 laboratory limit. The results illustrate that the NO_x emissions control of Vehicle B performed robustly well under real-world driving conditions. In terms of PN emissions, the PN EF of valid RDE trips was on average 5.5 times the China 6 PN limit, which suggests that Vehicle B would be unlikely to pass the RDE test if a PN CF of 2.1 is applied.

3.2.3 A comparison of RDE and laboratory test results

In the China 6 RDE regulation, the CFs of the whole trip and the urban segment separately are required to comply with the limits. Figure 10 presents the RDE test results by driving segment and the laboratory test results over the NEDC and the WLTP.

The average NO_x EF of RDE-valid tests of Vehicle A was in line with the WLTP test result, 1.7 times the China 5 limit and 14 times the NEDC test result. For Vehicle B, NO_x EFs of RDE and laboratory tests were all below the China 5 laboratory limit. NO_x emissions over the urban phase were always the highest of the three driving segments, except for RDE valid-II of Vehicle A – the NO_x emissions over motorway driving were the highest.

Vehicle A had totally different CO performances over the two valid RDE tests. As indicated by 12% higher CO₂ emissions (264 g/km versus 236 g/km), the RDE valid-I was much more aggressive than RDE valid-II. As a result, the CO EF of the RDE valid-I was 9.3 times the NEDC result, while that of RDE valid-II was at the same level as the NEDC test result. For Vehicle B, the CO emissions of valid RDE tests were on average 2.8 times the NEDC result and 31% lower than the result over the WLTP. In the China 6 RDE regulation, no limits have been set for CO emissions. Our test results provide a sound argument that CO emissions from gasoline cars can be high and are not

properly controlled under real-world driving conditions. Even though CO is not a major pollutant for urban air quality, it is toxic and affects human health. In addition, previous studies have demonstrated that CO emissions are in association with THC emissions (Yang, 2018). To include CO emissions in the RDE could generate reduction benefits of controlling VOC emissions and improvement in fuel injection control that may help mitigate particle emissions.

PN EFs of Vehicle B are substantially higher than those of Vehicle A. No PN limits are set for China 5 gasoline cars, so we plot the China 6 PN limit as a reference. PN EFs of three RDE trips of Vehicle A were all below the China 6 limit, indicating that particle emissions are not a major concern for PFI cars. However, PN EFs of Vehicle B under the NEDC, WLTC, and RDE tests were four to eight times the China 6 laboratory limit. This is a clear indication that PN emissions from GDI vehicles are very high and should receive special attention from regulators. In addition, it should be mentioned that the China 6 and the EU RDE legislation set a cut-off size of 23 nm for PN measurement, which means particles smaller than 23 nm are not detected and regulated. Recent research found that GDI engines can produce a significant share of nucleation mode of particles smaller than 23 nm (Giechaskiel and Martini, 2014). During a WLTP test, the number of sub-23 nm particles were on average 30%-40% of the total particle number for GDI engines (Giechaskiel and Martini, 2014). As a result, the actual PN emissions are not correctly counted under the current legislation. It was reported that particles of smaller dimensions might be more harmful to human health than bigger particles (Oberdörster et al. 2004). Therefore, it is essential to further study the particle size distribution from GDI engines and the technical feasibility of measuring sub-23 nm particles with PEMS PN measurement systems.

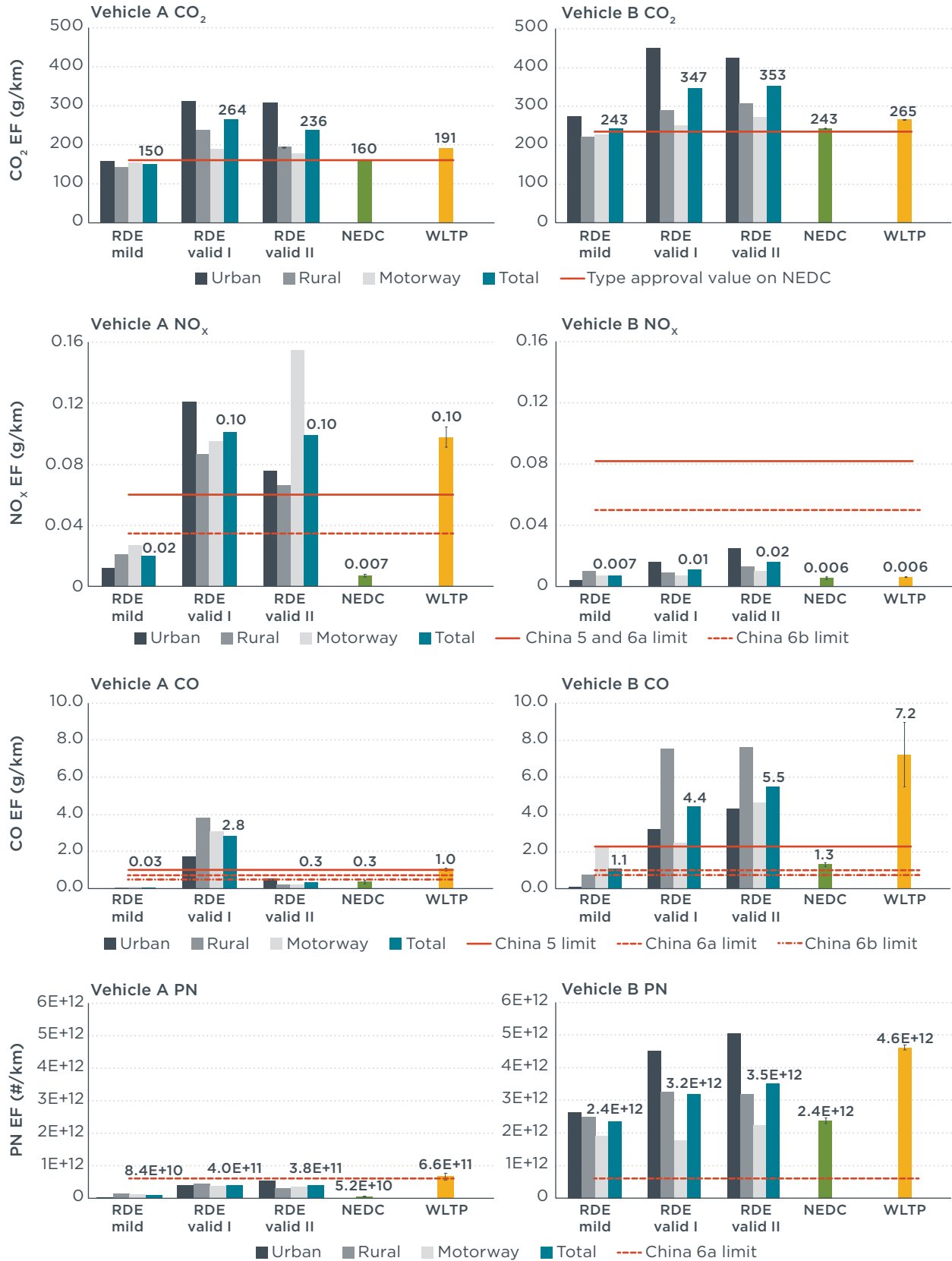


Figure 10 RDE and laboratory test results for CO₂, NO_x, CO, and PN emissions of Vehicles A and B

4 DISCUSSION

The discussion is subdivided into two sections, discussion of laboratory results and RDE results. We perform an in-depth analysis on the impacts of laboratory test conditions, including cold starts, driving cycles, different ambient temperatures, and A/C operation. For RDE tests, instantaneous emissions analysis is presented.

4.1 DISCUSSION OF LABORATORY RESULTS

4.1.1 Cold start versus hot start

Results in Figure 7 show that NO_x emissions from Vehicle A were compliant and well below the type-approval limit under the standard NEDC testing protocols with a cold start. However, NO_x emissions increased by more than 10 times on the same test starting with a hot engine. This behavior is inconsistent with the fact that emissions can be reduced easily once the engine and its after-treatment are warmed up, so a hot-start test should show much lower emissions for all pollutants.

To help understand the reasons for higher emissions during the hot-start test, Figure 11 compares the instantaneous NO_x emission rates in grams per second of the cold-start and hot-start tests on Vehicle A. NO_x emissions were comparable on both cold and hot tests and quite low during the first 60 seconds, becoming negligible after 140 seconds until the end of the test. The difference in the NO_x emissions occurred during a 70-second time frame of the test, starting around 60 seconds after the start.

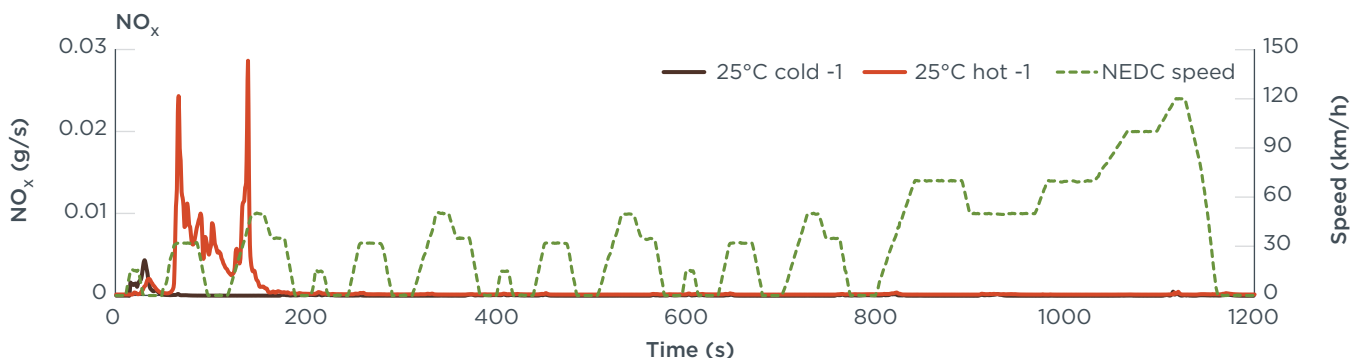


Figure 11 Instantaneous NO_x emission rates of Vehicle A under the cold and hot start NEDC

There are two primary potential causes of higher tailpipe NO_x emissions: 1) The light-off temperature of the TWC has not been reached and therefore it cannot convert pollutant emissions; 2) The light-off temperature of the catalyst is reached but there is no stoichiometric closed-loop control of the air-to-fuel mixture, which is required to convert efficiently engine-out NO_x emissions.

When the engine is started cold, most gasoline engines must apply a fast warm-up strategy for the catalyst to be able to reduce emissions in less than a minute after first ignition. Figure 12, Figure 13, and Figure 14 support that the vehicle applies typical fast catalyst warm-up strategies for the first 50 seconds after a start with a cold engine. Reduced spark advance read through the OBD port (see Figure 12) decreases the engine efficiency, resulting in higher exhaust temperatures. To maintain stable combustion during this initial idling phase, higher engine speeds are needed – 1,000 rpm instead of 800 rpm – as can be observed in Figure 13. The strategy more than doubles the

exhaust flow rate (Figure 14) and results in a much faster catalyst temperature rise for the cold-start test compared with a hot start, as shown on Figure 15. However, these strategies for cold start end after about 50 seconds and the TWC temperature after a hot start rapidly catches up after 50 seconds and is similar after about 60 seconds. As the catalyst temperatures are roughly the same after 60 seconds and are well above light-off temperature, catalyst temperature cannot be the cause of the major NO_x spikes that occurred up to 140 seconds.

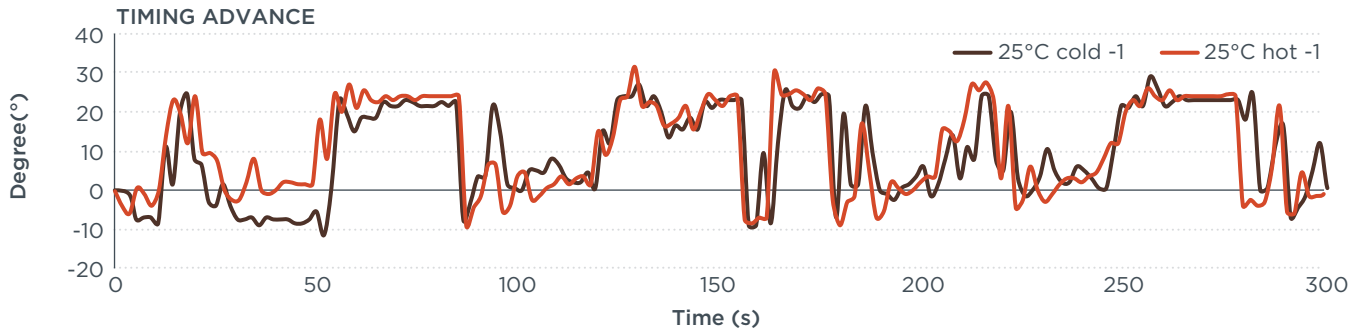


Figure 12 Spark advance of Vehicle A after hot and cold start NEDC tests

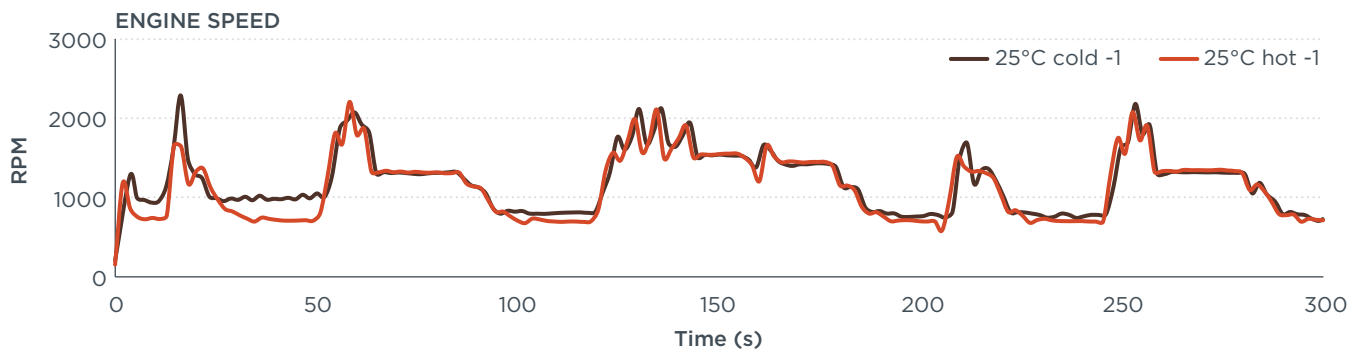


Figure 13 Engine speed of Vehicle A after hot and cold start NEDC tests

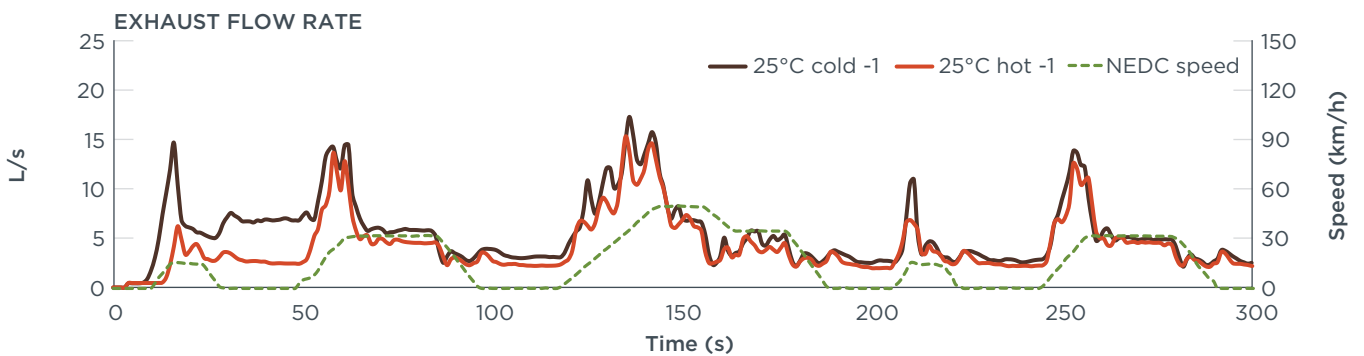


Figure 14 Exhaust flow rate of Vehicle A after hot and cold start NEDC tests

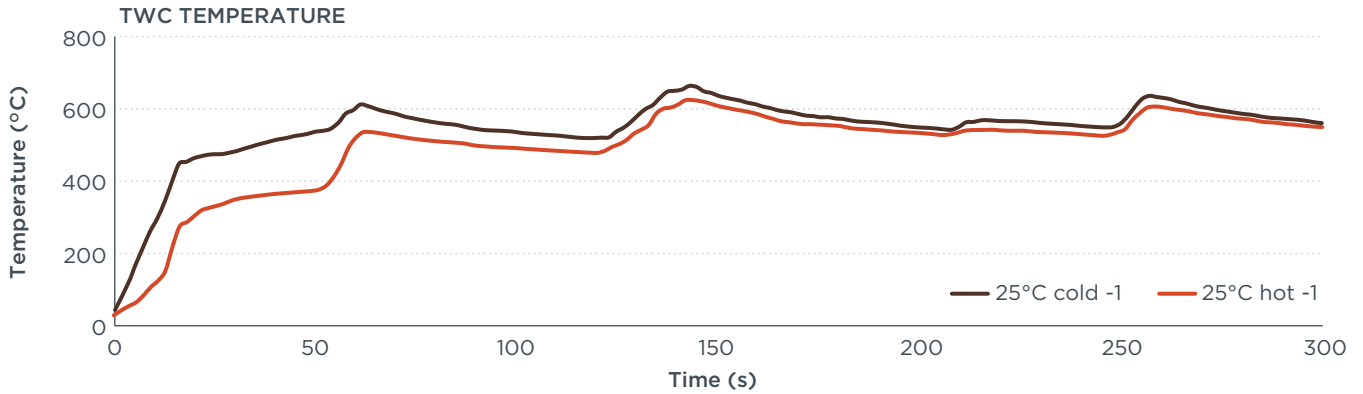


Figure 15 Exhaust temperature at the inlet of the catalyst of Vehicle A after hot and cold start NEDC tests.

TWCs need tight closed-loop control of the air-to-fuel mixture to efficiently convert emissions. The mixture has to run close to an ideal proportion of air and fuel (stoichiometric) in order to oxidize THC and CO emissions and reduce NO_x emissions simultaneously. To achieve such equilibrium, Vehicles A and B are equipped with dual O₂ sensors, one at the inlet of the catalyst and the other at the outlet. The O₂ sensors on Vehicles A and B are narrow-band sensors and cannot precisely identify the air-to-fuel ratio. Instead, the narrow-band sensor switches output voltage, indicating a lean or a rich air-to-fuel ratio.⁷ The engine’s Electronic Control Unit (ECU) uses the O₂ sensor signal to add or subtract fuel to keep the air/fuel mixture close to stoichiometry.

Figure 16 illustrates the difference of O₂ sensor voltage outputs between the cold and hot start test on Vehicle A, as read from the ECU through the OBD port. It is important to understand that narrow-band O₂ sensors cannot output more than 1.0 volt; thus, the ECU is not actually reporting the oxygen sensor voltage at the beginning of the tests. Instead, in the diagnostic test procedure, the ECU sends a signal >1.0 volt through the scan tool when the O₂ sensor is not ready. In Figure 16, it can be observed that the pre-catalyst sensor is ready in 15 seconds after a cold start, but it takes 130 seconds after a hot start. This indicates that the engine of Vehicle A was ignoring the O₂ sensor signal and running in open loop after a hot start for the first 130 seconds. A TWC – even hot – cannot reduce emissions correctly without a tight closed-loop control. This explains why NO_x emissions spikes were found during the hot start of Vehicle A. When the ECU was actively monitoring the O₂ sensor after 130 seconds and applying closed-loop mode, NO_x emissions rapidly dropped to almost zero (Figure 11).

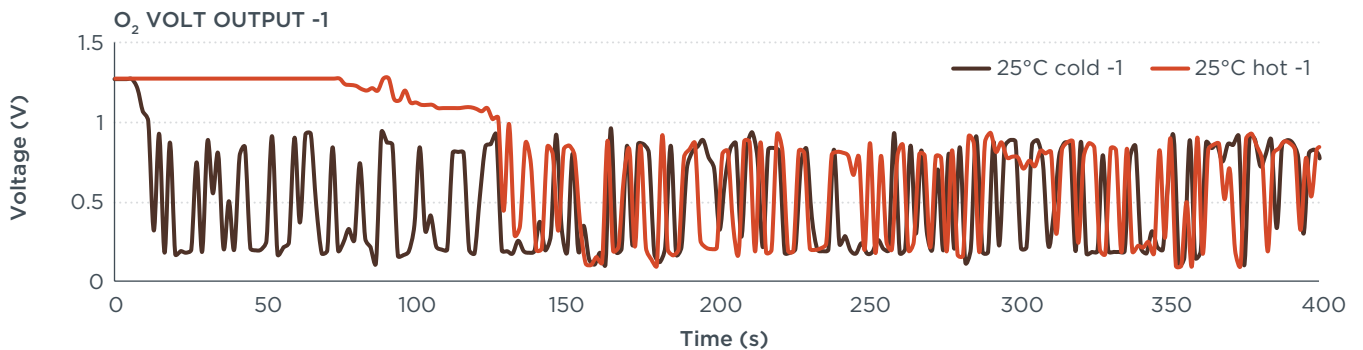


Figure 16 The inlet O₂ sensor voltage output at the OBD port of Vehicle A during the first 400 seconds under the cold and hot start NEDC

⁷ Narrow-band sensors are less costly than more accurate sensors known as wideband.

Figure 17 presents the instantaneous NO_x emissions rates of Vehicle B under the cold and hot start NEDC. NO_x emissions spikes were observed at the first 80 seconds after the cold start, especially during the first 40 seconds before catalyst light-off, and NO_x emissions were much lower after a hot start. In Figure 18, it can be observed that the ECU of Vehicle B began actively monitoring the O_2 sensor and entering closed-loop operation about the same time, 25 seconds, after a hot start and a cold start. These observations are what is expected from proper engine calibration.

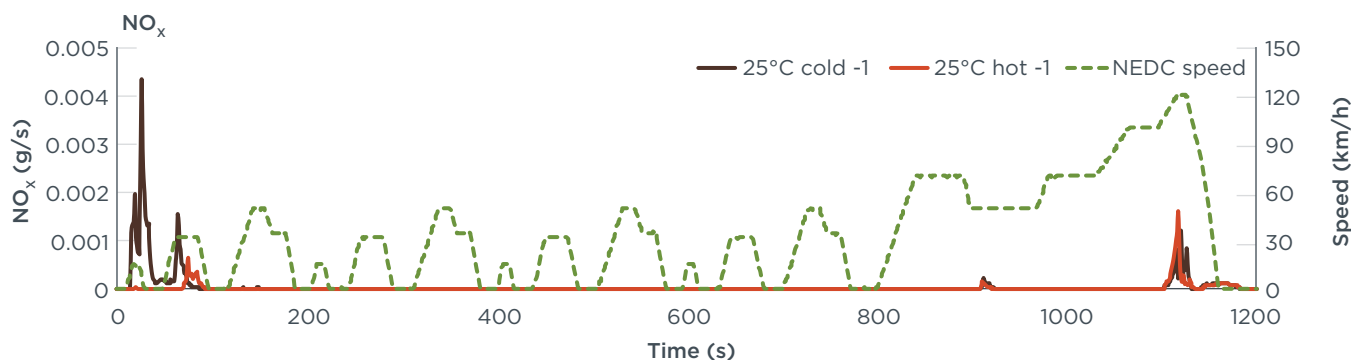


Figure 17 Instantaneous NO_x emission rates of Vehicle B under the cold and hot start NEDC

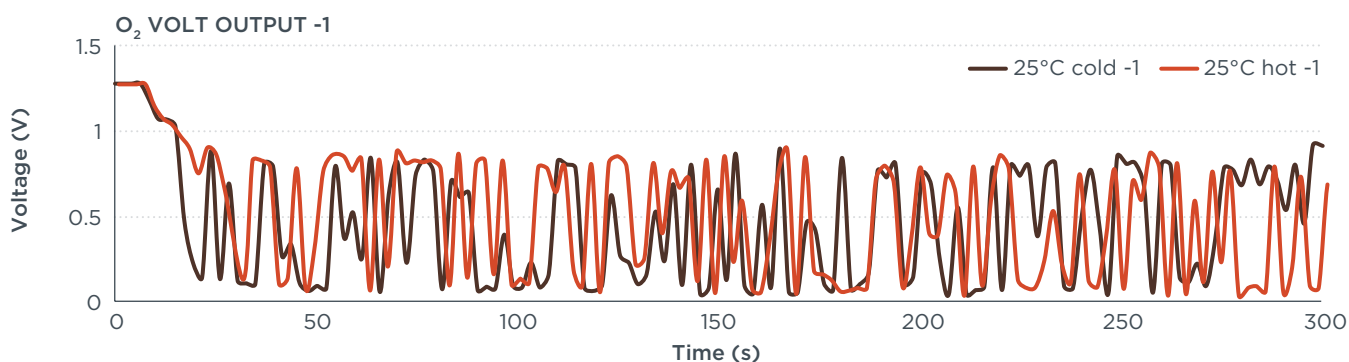


Figure 18 O_2 sensor voltage output at the inlet of Vehicle B during the first 300 seconds under the cold and hot start NEDC

These results suggest that Vehicle A had a lack of activation of its closed-loop control that prevented the TWC from controlling NO_x emissions. The results therefore suggest the lack of robustness of the emissions calibration on Vehicle A. The higher NO_x emissions that occurred during a hot start seem at least the consequence of a poor and lenient design of the injection and O_2 sensor control strategy on Vehicle A. Unfortunately, such an issue would not be detected during the test certification. That is because the actual certification protocol does not embed a hot soak test where the engine would have to start already warmed up.⁸ Such results demonstrate the importance for regulatory cycles to cover a wide variety of conditions that may happen in real-world driving conditions to prevent high off-cycle emissions.

4.1.2 WLTP versus NEDC

Vehicle A and Vehicle B had completely different NO_x performance but similar CO performance over standard WLTP tests (see Figure 19 and Figure 20). For Vehicle A,

⁸ The U.S. FTP-75 test integrates a stop of 10 minutes and a hot restart that covers this point.

NO_x EF over the WLTP test increased 13 times compared with results over the type-approval NEDC test, while Vehicle B had the same NO_x EFs over the two test procedures and both were much lower than the China 5 limit. CO emissions from both vehicles increased significantly moving from the NEDC to the WLTP.

For Vehicle A, NO_x spikes were found at around 1,700 seconds over the WLTP when the vehicle speed exceeded 120 km/h. For Vehicle B, no obvious high NO_x was observed during the whole test cycle. Elevated CO emissions were seen for both vehicles during the extra high-speed phase of the WLTP, at around 1,600 to 1,800 seconds. In Figure 21, we can see that the engine load of both vehicles reached full load during the extra high-speed phase of the WLTP, the same time period when CO spikes were observed. Given that CO is a pretty good surrogate for rich air-to-fuel ratio, the results suggest that both vehicles were going rich at high engine loads to increase power during hard accelerations and/or to cool the engine and the catalyst to prevent damage.

A recent testing program on 12 Euro 5 and Euro 6 gasoline cars in Europe reported that moving from the NEDC to the WLTP did not have a clear impact on NO_x emissions but significantly increased the CO emissions (Marotta, Pavlovic, Ciuffo, Serra, and Fontaras, 2015). The results for Vehicle B were consistent with the previous findings, but Vehicle A seemed to be an outlier. The unusual high NO_x emissions from Vehicle A might be attributed to a poor design of the air-to-fuel ratio control strategy, as discussed in the previous section.

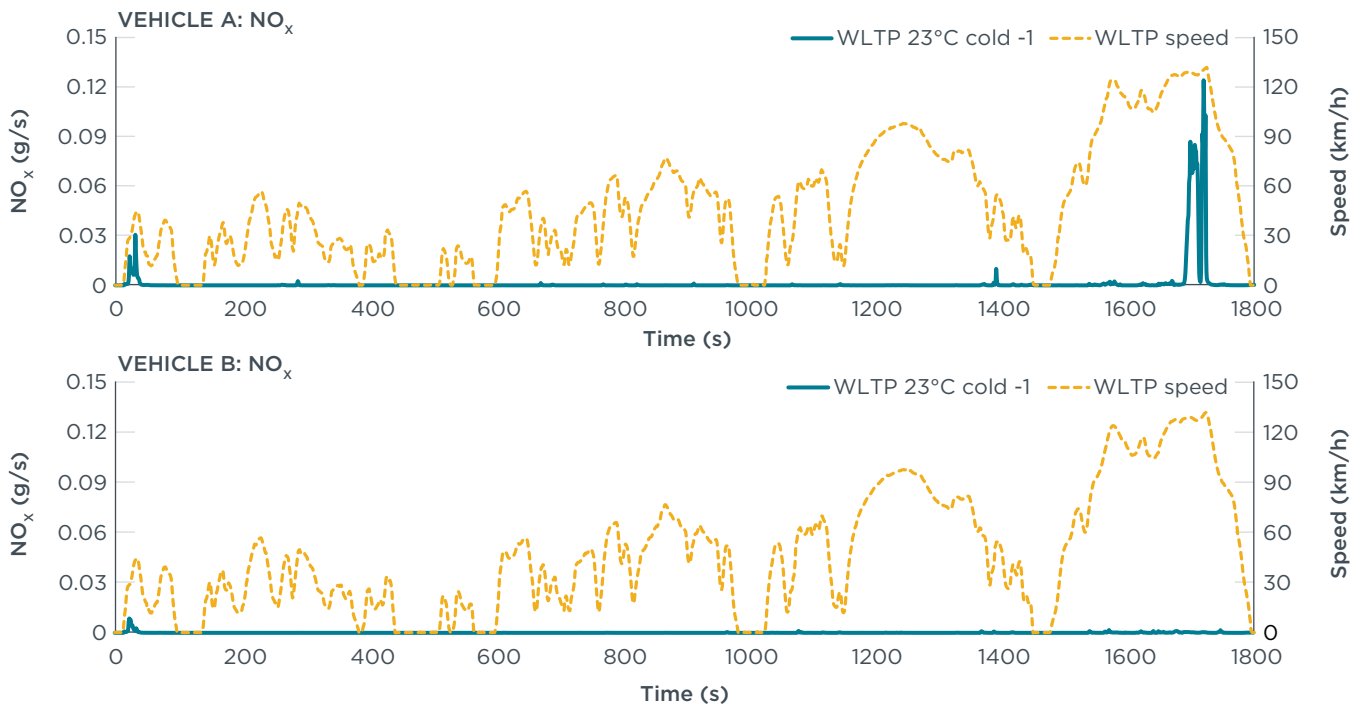


Figure 19 Instantaneous NO_x emission rates of Vehicles A and B over the standard WLTP test

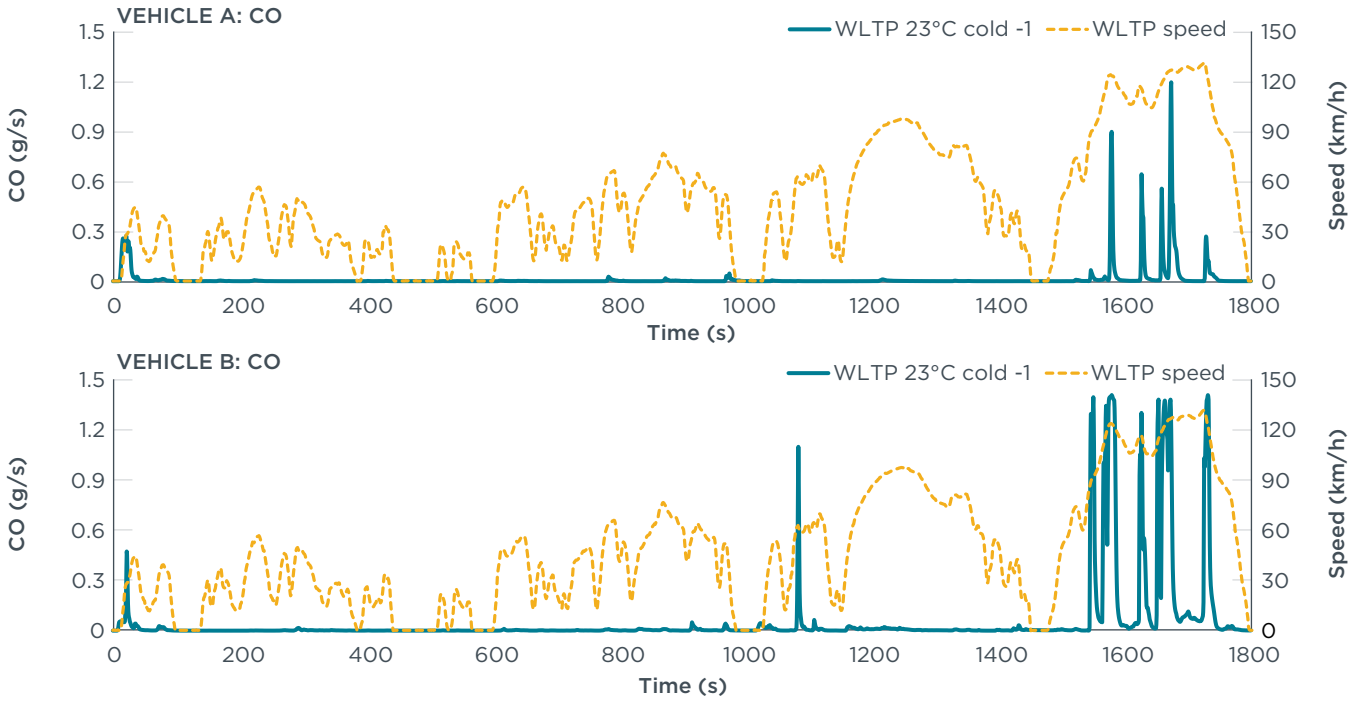


Figure 20 Instantaneous CO emissions rates of Vehicles A and B over the standard WLTP test

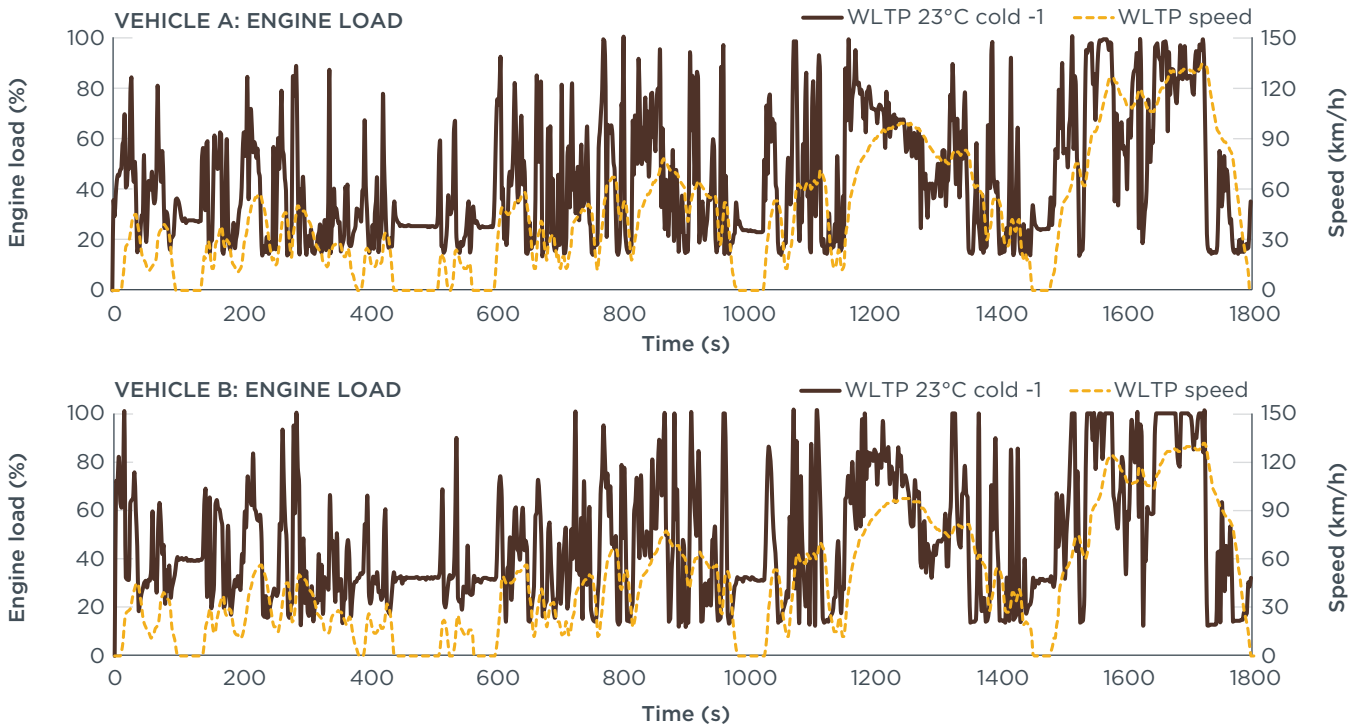


Figure 21 Instantaneous engine load of Vehicles A and B over the standard WLTP test

4.1.3 Different ambient temperature

Vehicle A was tested over the NEDC cold start at 14°C, 25°C, and 30°C. The highest NO_x, CO, and THC emissions were found at 14°C, the lowest temperature. The NO_x, CO, and THC EFs at 14°C were 100%, 25%, and 270% higher than the values at 30°C. The results are consistent with expectations, as the colder engine took longer to warm up (see Figure 23) and needs longer enrichment after the start. In addition, there were no increases in emissions after the engine warmed up at 100 seconds, indicating that everything was operating as it should have been.

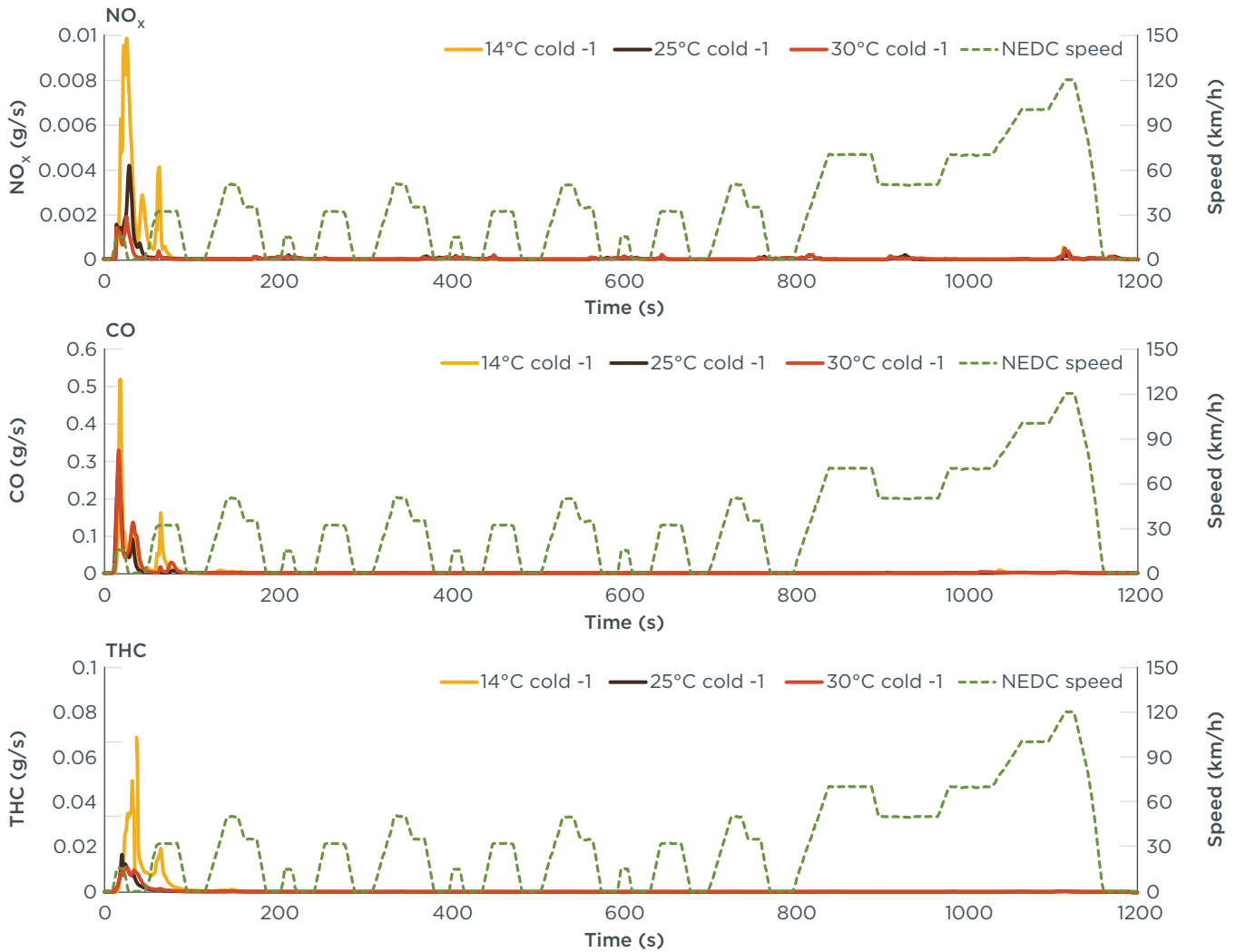


Figure 22 Instantaneous NO_x, CO, and THC emission rates of Vehicle A over the NEDC at 14°C 25°C, 30°C

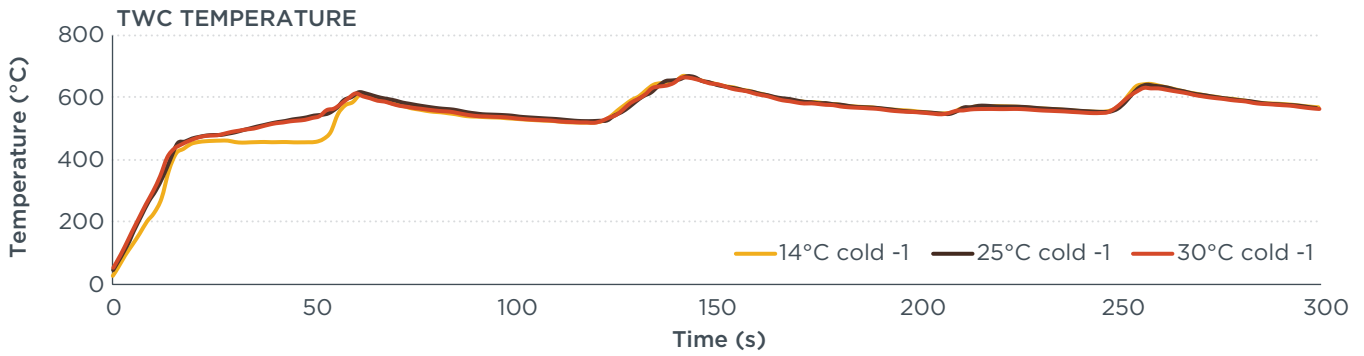


Figure 23 Instantaneous TWC temperature of Vehicle A at first 300 seconds over the NEDC at 14°C, 25°C, and 30°C

4.1.4 A/C on versus A/C off

Figure 24 and Figure 25 show the impacts of A/C on and A/C off on NO_x and CO emissions rates of Vehicle A over the NEDC 30°C and the WLTP 30°C. The impacts of A/C were inconsistent over different driving cycles. When A/C was turned on, NO_x EF increased 100% over the NEDC, while it decreased 50% over the WLTP. CO emissions stayed at the same level over the NEDC, while increasing 75% over the WLTP. Over the NEDC, NO_x and CO spikes were seen only in the first 50 seconds of cold start. But over the WLTP, elevated NO_x and CO emissions occurred from 1,600 to 1,800 seconds during the extra high-speed phase of the WLTP.

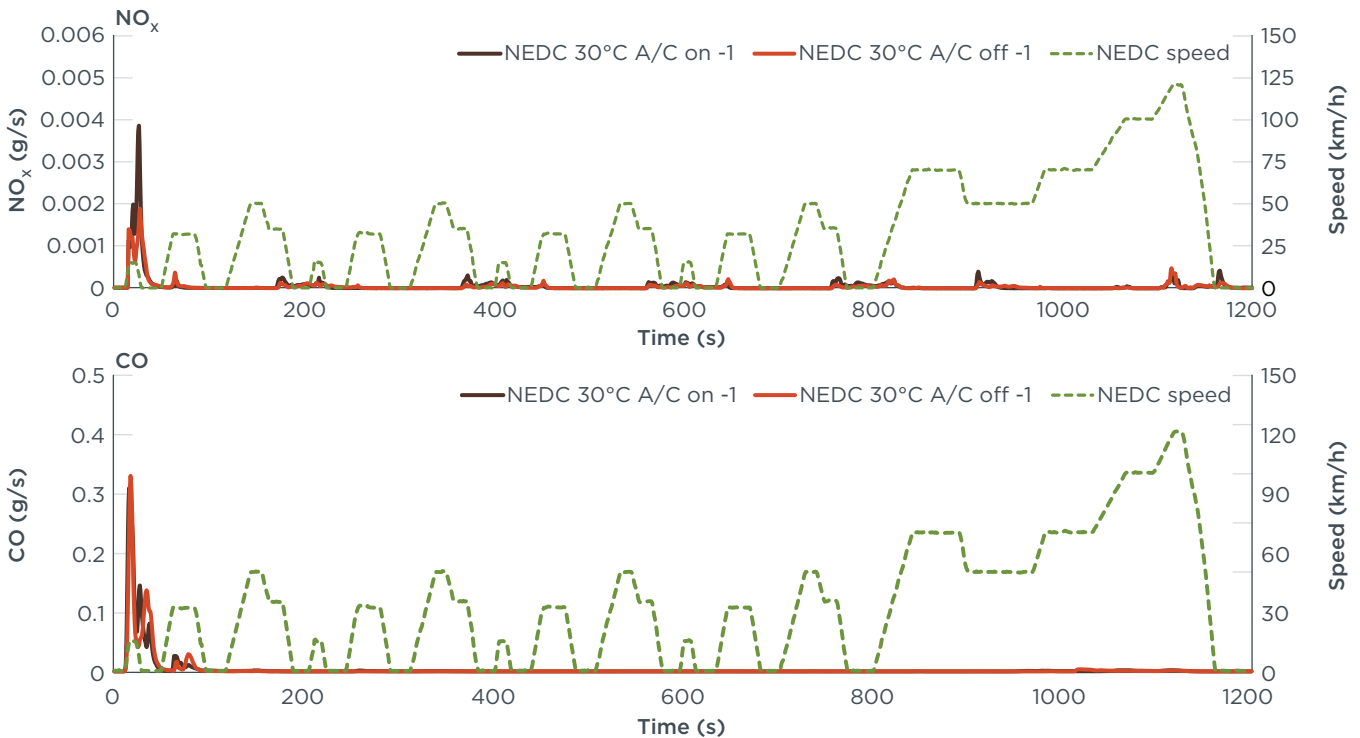


Figure 24 Instantaneous NO_x and CO emissions rates of Vehicle A over the NEDC at 30°C with A/C on and off

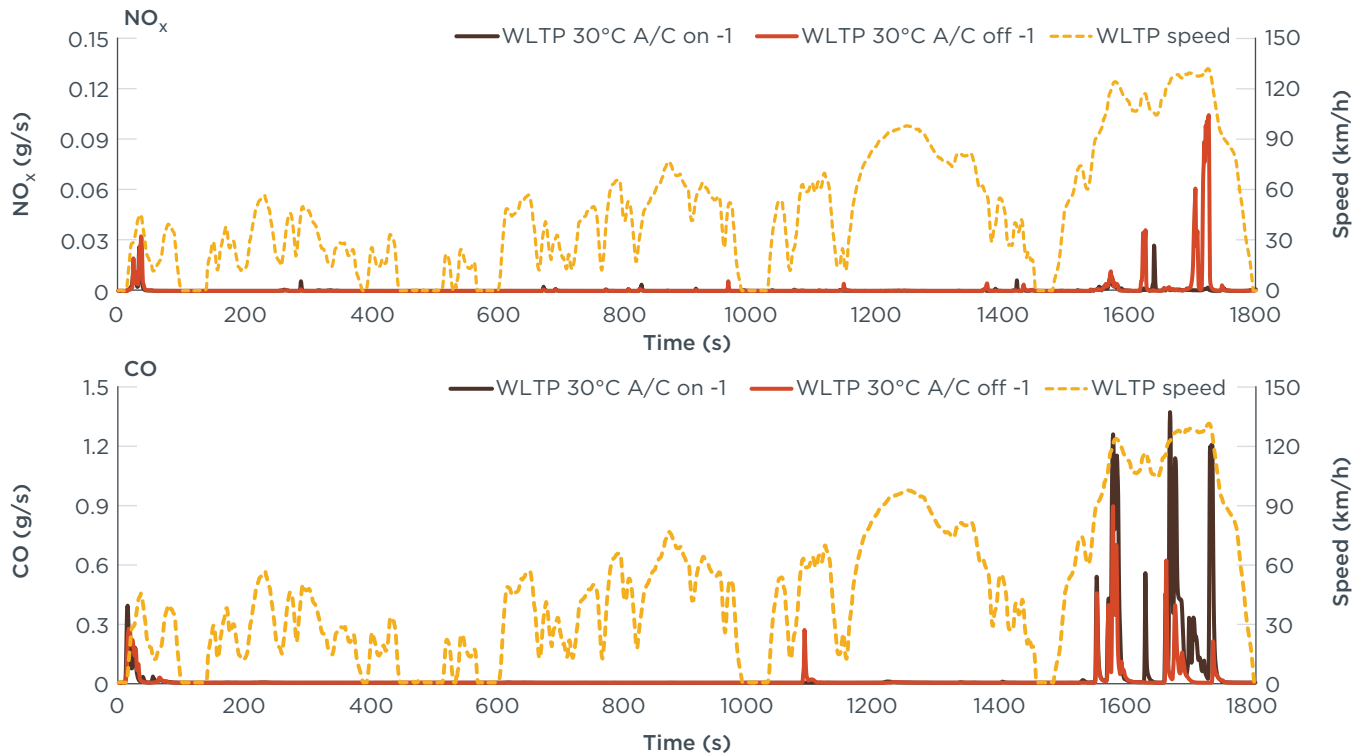


Figure 25 Instantaneous NO_x and CO emissions rates of Vehicle A over the WLTP at 30°C with A/C on and off

By looking at the instantaneous engine loads over the NEDC (see Figure 26), it can be observed that the engine load with A/C on was always higher than with A/C off. However, results over the WLTP (see Figure 27) illustrate that the engine load during the high-speed phase of the WLTP with A/C on and off both reached the full load. As a result, higher load demands from the compressor may be pushing the operation to richer conditions, and richer operation increases CO emissions and reduces engine-out NO_x .

Previous studies demonstrated that the relationship of A/C operation and emissions is a complex issue. Welstand, Haskew, Gunst, and Bevilacqua (2003) reported that the operation of A/C resulted in consistent increases in CO and NO_x over the U.S. test cycle. Weilenmann, Vasic, Stettler, and Novak (2005) tested six gasoline cars in Europe and found that CO and THC notably increased with A/C on, but the trend in NO_x was quite small. The emissions are influenced by temperature, humidity, solar load and A/C technologies (Welstand et al., 2003). Further research is needed to evaluate all these factors.

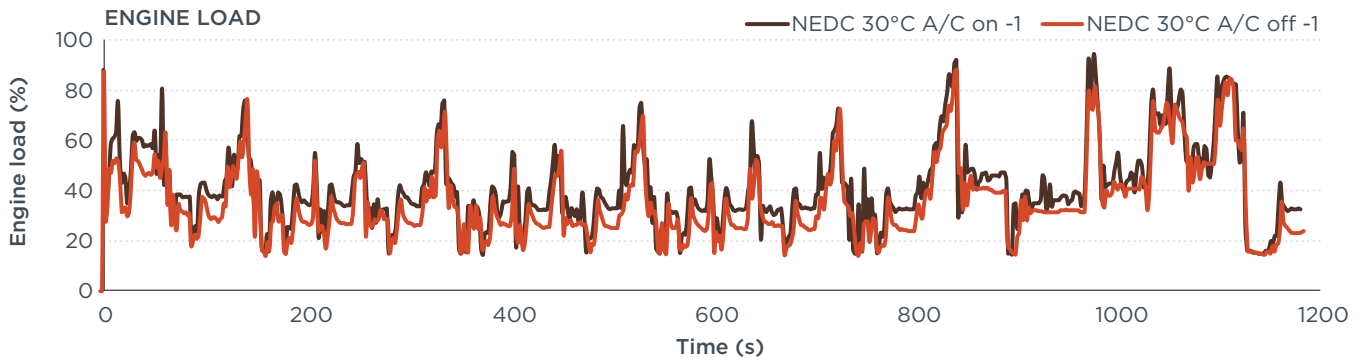


Figure 26 Instantaneous engine load of Vehicle A over the NEDC at 30°C with A/C on and off

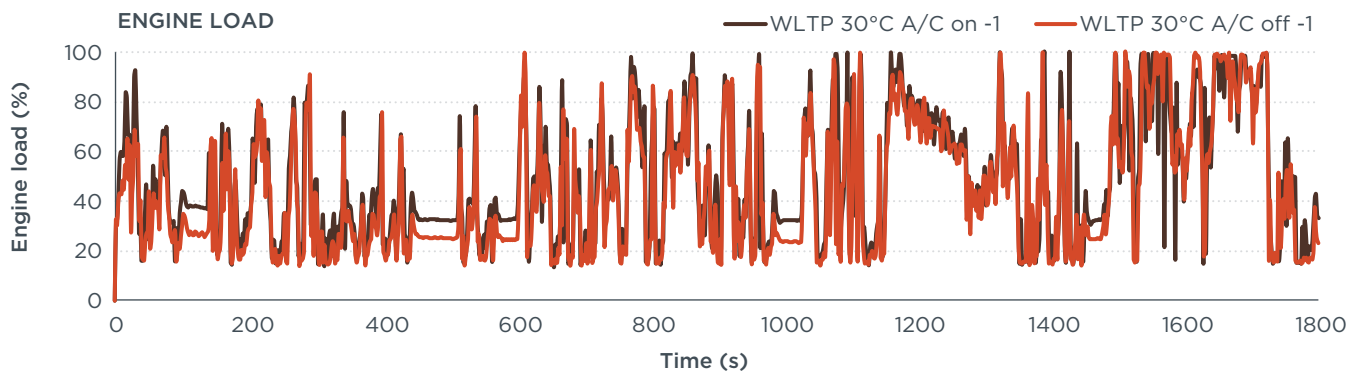


Figure 27 Instantaneous engine load of Vehicle A over the WLTP at 30°C with A/C on and off

4.1.5 Particle emissions from GDI vehicle

In laboratory testing, second-by-second PM measurement was not available. Figure 28 and Figure 29 show the instantaneous PN concentration of Vehicle B over the NEDC cold start, NEDC hot start, and WLTP cold start. PN spikes were seen during the first 300 seconds of cold starts, the high-speed phase of the NEDC, and the extra high-speed phase of the WLTP. This indicates that PN emissions from GDI cars are mostly generated when the engine is not warmed up (the first 300 seconds in the NEDC) and during transient and aggressive driving conditions. As a result, PN emissions over the NEDC cold start were 1.6 times those over a hot start, and PN emissions were almost twice as high if the test cycle was shifted from the NEDC to the WLTP. The results add to the growing evidence that PN emissions from current technology GDI vehicles are significant (Fu et al., 2014; Badshah et al., 2016; Chen, Liang, Zhang, and Shuai, 2017). This study highlights a clear need for better controlling particle emissions from GDI vehicles to comply with the China 6 PN standard.

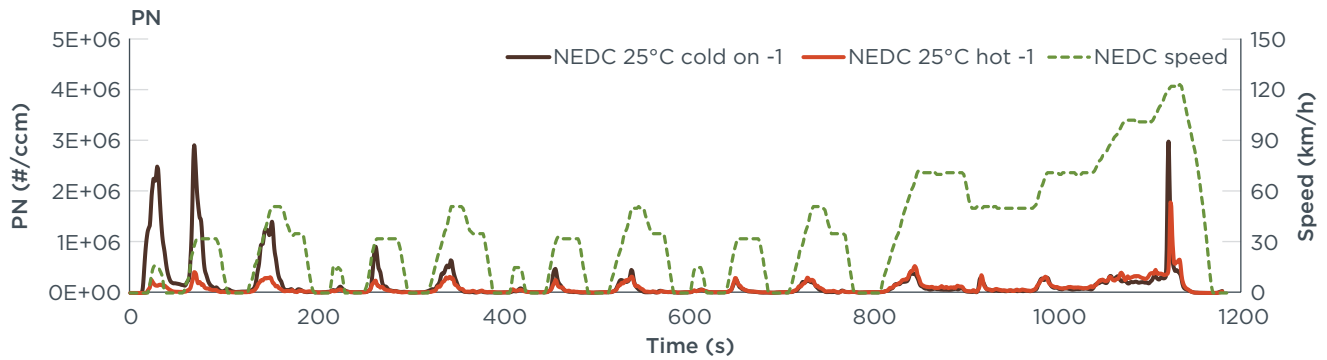


Figure 28 Instantaneous PN concentration of Vehicle B over the NEDC cold and hot start

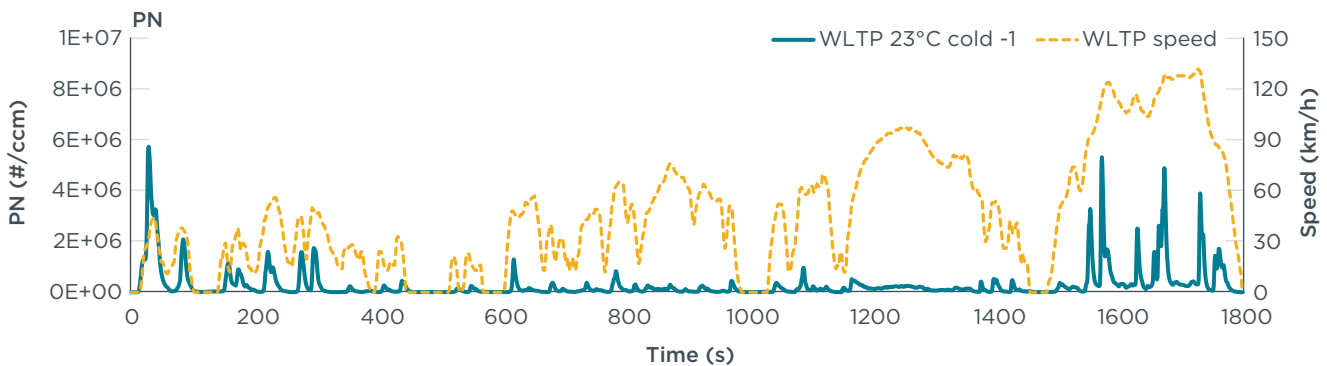


Figure 29 Instantaneous PN concentration of Vehicle B over the WLTP cold start

4.2 DISCUSSION OF RDE RESULTS

In this section, we take the first valid RDE trip of Vehicle A and Vehicle B as examples and perform an in-depth analysis on instantaneous emissions.

To further examine the emissions performance of the two trips, we plotted the instantaneous emissions rates of NO_x , CO, and PN, and instantaneous velocity (see Figure 30 and Figure 31). It can be observed that the driving profiles of the two trips were similar. The urban, rural, and motorway phases can be clearly distinguished.

The highest NO_x emissions peak of Vehicle A occurred at the first 50 seconds. By checking the instantaneous engine coolant temperature signal, we found that the initial engine coolant temperature of this trip was 82°C. In the China 6 RDE regulation, the cold start period ends once the coolant has reached 70°C for the first time but no later than five minutes after initial engine start. Therefore, the RDE valid-I of Vehicle A was not a cold start according to the regulation. The high NO_x emissions during the hot-start period was similar to the performance under the NEDC hot start in laboratory testing. In addition, plenty of NO_x peaks were observed during the whole trip. Unfortunately, O_2 sensor voltage outputs were not available in the PEMS test for further investigation, but the high NO_x emissions of Vehicle A appear to be attributed to poor emissions calibration during stronger accelerations than occur on the NEDC. CO spikes were mostly observed during rural and motorway driving. PN emissions of Vehicle A stayed at a relatively low level during the whole trip.

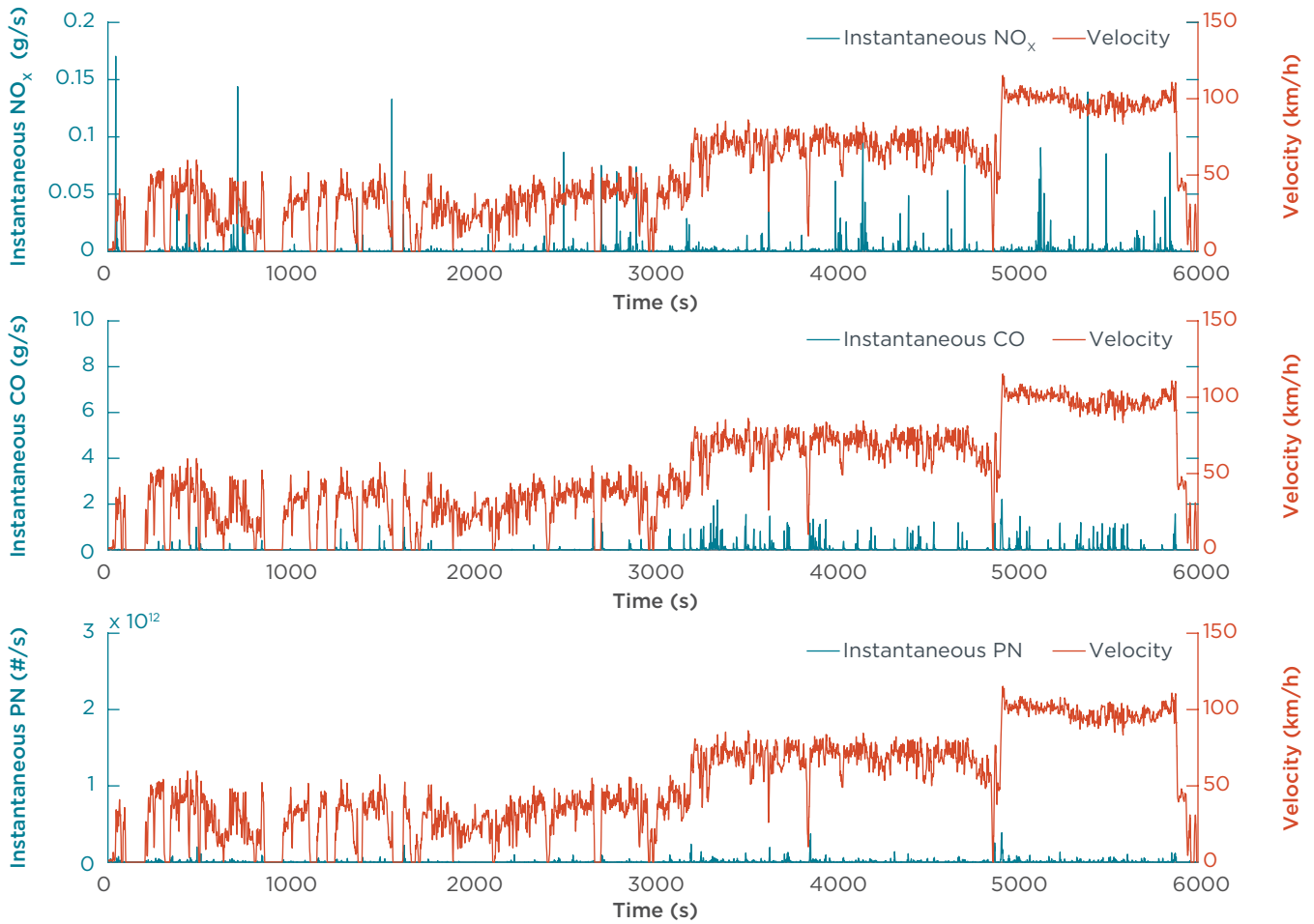


Figure 30 Instantaneous emissions rates (NO_x , CO, PN) and vehicle velocity of Vehicle A RDE valid-I

For Vehicle B, NO_x emissions were well controlled during the whole trip, with NO_x spikes hardly seen, while several CO peaks were found during rural and motorway driving. As discussed before, CO is primarily a function of air-to-fuel enrichment, which means high CO usually occurs at rich events. The results illustrate that the vehicle was running rich during accelerations in rural and motorway driving. Significant high PN emissions were observed throughout the trip, with spikes corresponding to enrichment during accelerations. It further demonstrates that the high PN emissions from GDI cars could be very high and deserve special attention from regulators.

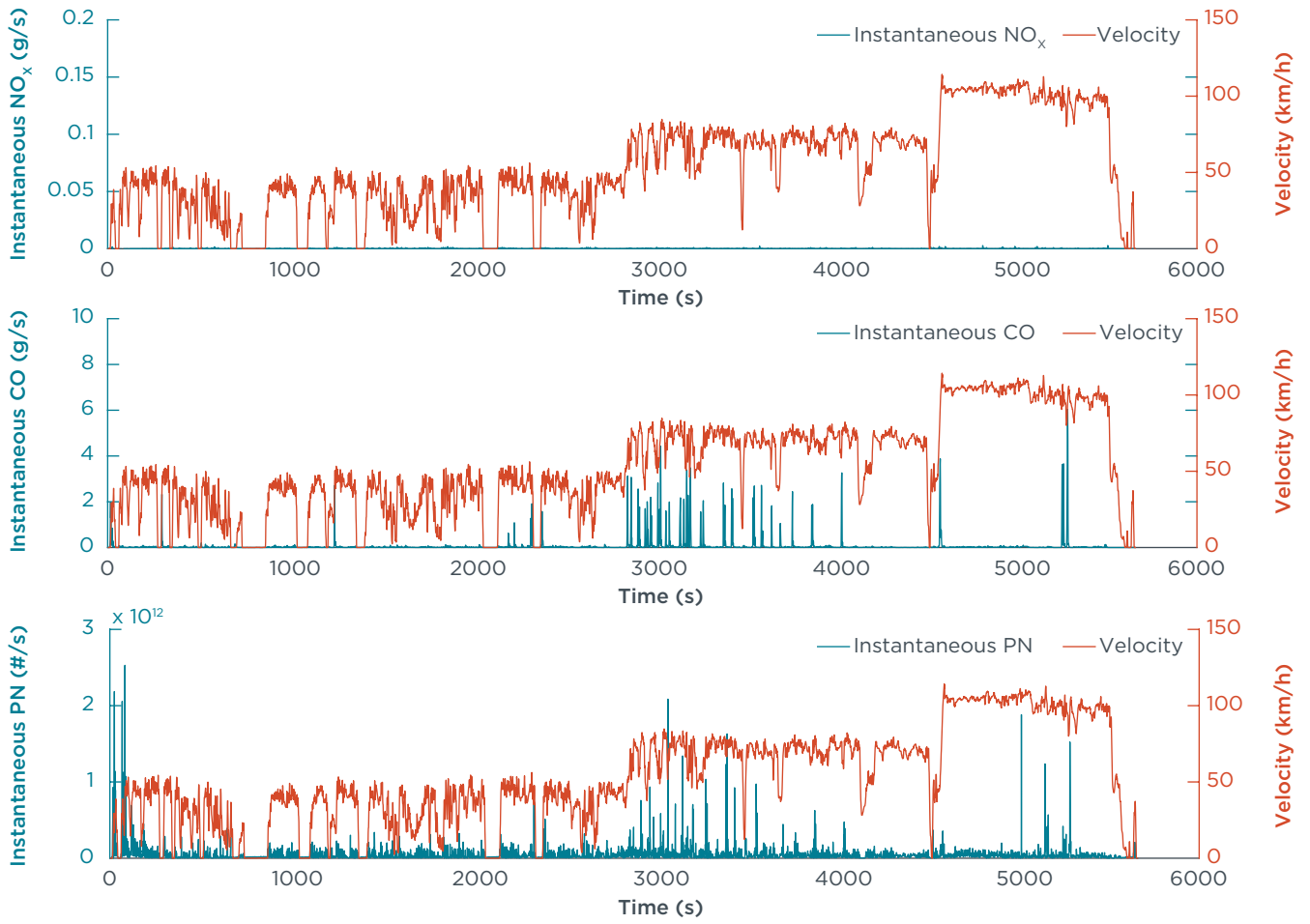


Figure 31 Instantaneous emissions rates (NO_x , CO, PN) and vehicle velocity of Vehicle B RDE valid-I

5 CONCLUSIONS AND POLICY RECOMMENDATIONS

5.1 CONCLUSIONS

In this report, two China 5 gasoline cars were tested under laboratory and on-road driving conditions. Vehicle A was a Type 1 small car equipped with PFI engine, and Vehicle B was a Type 2 GDI multi-purpose vehicle. In laboratory tests, we conducted the regulatory NEDC type-approval test and enhanced tests under modified conditions. In on-road tests, both vehicles were tested on the same RDE-compliant routes.

Test results suggest that vehicles certified as compliant under the NEDC type-approval protocol may have high emissions under more representative testing procedures in laboratory and in real-world driving. This study provides a sound argument that the current NEDC-based testing framework is insufficient to control real-world emissions from LDVs in China.

Under the NEDC type-approval protocol, NO_x , CO, THC, and PM emissions of both vehicles stayed below regulatory limits. However, under modified laboratory testing conditions, emissions could be significantly elevated. It is widely known that gasoline vehicle emissions can be easily controlled with a warmed-up engine and a three-way catalyst, so emissions under hot starts should be much lower than the results under cold starts. In most cases of this study, NO_x , CO, THC, PM, and PN emissions under hot starts were lower than those under the same test cycle and conditions with cold start. The only exception was that the NO_x EF of Vehicle A under the NEDC hot start was 10 times the result under the same test with cold start. Our in-depth investigation into O_2 sensor voltage shows that the higher NO_x emissions during a hot start were attributed to a poor and lenient design of the air-to-fuel ratio control strategy on Vehicle A. To avoid this situation, the RDE 3rd package in the European Union introduced a provision that asks OEMs to test under cold start but also hot start in a minimum number of cases per vehicle PEMS test family. Unfortunately, such high emissions cannot be detected in the current certification protocol in China. Also, the NO_x emissions of Vehicle A over a standard WLTP test was 13 times higher than over a standard NEDC and 1.7 times the China 5 limit. This indicates that Vehicle A would not pass the type-approval test if the driving cycle is changed to the WLTP, as it does in the China 6 standard. The findings highlight the importance for regulatory tests to cover representative test cycles and conditions to prevent high off-cycle emissions.

CO emissions of both vehicles stayed below the China 5 limit under all NEDC tests, while they failed to pass the tests under the WLTP. In addition, CO emissions of both vehicles over valid RDE tests exceeded the laboratory limits by 1.9 to 2.8 times. The test results imply that CO emissions from gasoline vehicles can be significantly higher in real-world driving, due primarily to enrichment during acceleration. Nevertheless, the China 6 RDE regulation has not set a CO limit. Introducing CO limits in the China 6 RDE regulation is much needed to further control CO emissions from gasoline cars. In gasoline vehicles, HC and particulate emissions tend to be strongly correlated with enrichment, so controlling CO emissions would limit enrichment and correspondingly reduce HC and particulate emissions.

THC emissions are compliant with the standard under all laboratory test conditions except for the test over the NEDC at 14°C cold start of Vehicle A. Tailpipe THC emissions from gasoline rose under low ambient temperatures but were generally effectively controlled thanks to the aftertreatment device.

PN emissions from the GDI vehicle, Vehicle B, were significantly high under both laboratory and RDE tests. In the China 5 standard, no PN limits have been set for gasoline vehicles. If we take the China 6 PN limit as a reference, PN emissions of the GDI car were four times the limit over the standard NEDC test, eight times over the standard WLTP, and 5.5 times over the RDE tests. These findings support the idea that PN emissions from current GDI cars can be very high and should be further controlled with implementation of new standards.

In terms of particulate emissions, PM emissions from the two vehicles all managed to stay below the China 5 and 6 limits under laboratory tests.

5.2 POLICY RECOMMENDATIONS

This testing project is the first third-party-run RDE testing program in China and provides a good basis for further study of real-world emissions from LDVs. The findings from this study point to several policy implications related to emissions standards and in-use compliance programs in China.

The new China 6 LDV standard, which will take effect July 1, 2020, is a significant step toward effectively controlling real-world emissions from LDVs in China. Unlike previous standards, the China 6 combines best practices from both European and U.S. regulations in addition to creating its own provisions. Major improvements include shifting from the NEDC to the WLTP, adoption of RDE testing requirements for both type test and in-use conformity, and the most comprehensive ever in-use compliance program. Under the new testing framework, manufacturers will have to demonstrate that vehicles show compliance with emissions limits not only in the laboratory tests but also in real-world driving throughout the vehicle's useful life. We believe the new China 6 standard will bring tremendous emissions reductions and air quality benefits with effective implementation. Thus, at the local level, we recommend that:

1. Provinces and cities facing severe air pollution implement the China 6 standard as early as possible.

In the laboratory tests, we found that gaseous and particulate emissions under cold starts were significantly higher than those under hot starts in most cases. Previous studies have demonstrated that cold start is an important contributor to vehicle emissions, especially in urban areas (Wang et al., 2010; Fu et al., 2014; Weiss et al., 2017). In northern China where residents experience terrible winter haze events, the issue of cold starts can be critical. Unfortunately, the China 6 RDE regulation does not include cold-start operation in the data evaluation process. The China 6 RDE primarily followed the Euro 6 RDE Package 2 passed in April 2016, which excluded cold starts in the data evaluation process. After consultation and discussion with stakeholders, the European Commission approved including cold-start emissions in the third RDE Package in December 2016. The inclusion of cold starts in the RDE requirements will be essential for ensuring the use of improved emissions control technologies and controlling real-world emissions. Thus, we recommend that China:

2. Conduct further investigation of cold-start frequencies and trip distances in China.
3. Conduct further studies on the impacts of cold starts in future RDE testing programs.
4. Include cold starts in the RDE regulation as soon as possible, while maintaining a minimum number of hot start tests like the RDE 3rd package provisions in the European Union.

The experimental results in this study suggest that CO from gasoline cars could be substantial under more representative driving conditions in laboratory and real-world driving. However, no CO limits have been set in the China 6 RDE regulation. CO limits were not introduced in the EU RDE regulation mainly because CO emissions are mostly generated from gasoline cars, while diesel cars account for more than 50% of the European passenger vehicle market (the ICCT, 2017).⁹ In China, around 97% of LDVs are powered by gasoline. Even though CO is not a major pollutant for urban air quality, it is toxic and affects human health. In addition, previous studies have demonstrated that THC and CO emissions tend to rise and fall together (Yang, 2018). Limiting CO emissions could indirectly limit THC emissions that contribute toxic emissions and secondary organic aerosol in the atmosphere and could improve fuel injection control that may help mitigate particle emissions. Thus, we recommend that China:

5. Add CO requirements to the RDE regulation as soon as possible.

To further control particle emissions from the growing number of GDI vehicles, the China 6 RDE regulation has set a PN CF of 2.1. This means the PN emissions in real-world driving should not exceed the laboratory limit by more than 2.1 times. In the European Union, a PN CF of 1.5 has been introduced based on the analysis of the uncertainty introduced by PEMS testing. Thus, we recommend that China:

6. Set a timeline for adoption of a CF of 1.5 for PN emissions under RDE testing.

Sub-23 nm particles, reported to account for a large percentage of particles from gasoline engines, are not measured and regulated in the China 6 standard. Considering that small particles might be more harmful than bigger particles to human health, we recommend that China:

7. Conduct further investigation of particle size distribution from gasoline engines and study the technical feasibility of measuring sub-23 nm particles without affecting the uncertainty of PN measurement systems.

Recently, the Chinese government has made substantial efforts on vehicle emissions compliance and enforcement. China's new Air Pollution Prevention and Control Law, which took effect January 1, 2016, gave the MEE clear authority to enforce the emissions standards and penalize noncompliance. Manufacturers are required to test their vehicles and report the test results to the MEE. The agency has the authority to randomly test in-use vehicles. On-road PEMS testing is an excellent tool for in-use compliance programs, but it requires a high level of resources, including sophisticated equipment, professional technicians, and high cost. The enhanced laboratory testing conducted in this study can serve as a simplified tool for identifying high emitters and screening defeat devices. Various testing conditions in enhanced laboratory testing include cold and hot starts, various ambient temperatures, and modified driving cycles. Higher emissions over the non-regulatory test protocols may indicate lack of robustness of emissions calibration or a defeat device strategy. We recommend that:

8. The MEE and local agencies consider enhanced laboratory testing as a simplified pre-screening method for the in-surveillance program.

⁹ From communication with European Commission Joint Research Center.

REFERENCES

- Badshah, H., Kittelson, D., & Northrop, W. (2016). Particle emissions from light-duty vehicles during cold-cold start. *SAE International Journal of Engines*, 9(3), 1775-1785. Retrieved from <https://doi.org/10.4271/2016-01-0997>
- Carlaw, D. C., Beevers, S. D., Tate, J. E., Westmoreland, E. J., & Williams, M. L. (2011). Recent evidence concerning higher NO_x emissions from passenger cars and light duty vehicles. *Atmospheric Environment*, 45(39), 7053-7063. Retrieved from <https://doi.org/10.1016/j.atmosenv.2011.09.063>
- Carlaw, D. C., & Rhys-Tyler, G. (2013). New insights from comprehensive on-road measurements of NO_x, NO₂ and NH₃ from vehicle emission remote sensing in London, UK. *Atmospheric Environment*, 81, 339-347. Retrieved from <https://doi.org/10.1016/j.atmosenv.2013.09.026>
- Chen, L., Liang, Z., Zhang, X., & Shuai, S. (2017). Characterizing particulate matter emissions from GDI and PFI vehicles under transient and cold start conditions. *Fuel*, 189, 131-140. Retrieved from <https://doi.org/10.1016/j.fuel.2016.10.055>
- Cui, H., Chen, W., Dai, W., Liu, H., Wang, X., & He, K. (2015). Source apportionment of PM_{2.5} in Guangzhou combining observation data analysis and chemical transport model simulation. *Atmospheric Environment*, 116, 262-271. Retrieved from <https://doi.org/10.1016/j.atmosenv.2015.06.054>
- European Commission. (2016a). Commission Regulation (EU) 2016/427 of 10 March 2016 amending Regulation (EC) No 692/2008 as regards emissions from light passenger and commercial vehicles (Euro 6). Retrieved from <http://eur-lex.europa.eu/legal-content/EN/TXT/PDF/?uri=CELEX:32016R0427&from=EN>
- European Commission. (2016b). Commission Regulation (EU) 2016/646 of 20 April 2016 amending Regulation (EC) No 692/2008 as regards emissions from light passenger and commercial vehicles (Euro 6). Retrieved from <http://eur-lex.europa.eu/legal-content/EN/TXT/PDF/?uri=CELEX:32016R0646&from=EN>
- Franco, V., Posada Sánchez, F., German, J., & Mock, P. (2014). *Real-world exhaust emissions from modern diesel cars*. The International Council on Clean Transportation: Washington, DC. Retrieved from <http://www.theicct.org/real-world-exhaust-emissions-modern-diesel-cars>
- Fraser, N., Blaxill, H., Lumsden, G., & Bassett, M. (2009). Challenges for increased efficiency through gasoline engine downsizing. *SAE International Journal of Engines*, 2(1), 991-1008. Retrieved from <https://doi.org/10.4271/2009-01-1053>
- Fu, H., Wang, Y., Li, X., & Shuai, S. (2014). Impacts of cold-start and gasoline RON on particulate emission from vehicles powered by GDI and PFI engines. *SAE Technical Paper*, 2014-01-2836. Retrieved from <https://doi.org/10.4271/2014-01-2836>
- Giechaskiel, B. & Martini, G. (2014). *Review on engine exhaust sub-23 nm particles*. (JRC Science and Policy Report). Retrieved from <https://doi.org/10.2790/22597>
- Hall, D. & Dickens, C. (1999). Measurement of the number and size distribution of particles emitted from a gasoline direct injection vehicle. *SAE Technical Paper*, 1999-01-35(724). Retrieved from <https://doi.org/10.4271/1999-01-3530>

- Huang, R. J., Zhang, Y., Bozzetti, C., Ho, K. F., Cao, J. J., Han, Y., ... Prévôt, A. S. H. (2014). High secondary aerosol contribution to particulate pollution during haze events in China. *Nature*, 514(7521), 218–222. Retrieved from <https://doi.org/10.1038/nature13774>
- The International Council on Clean Transportation (ICCT). (2017). *European Vehicle Market Statistics Pocketbook 2017/18*. Retrieved from http://eupocketbook.org/wp-content/uploads/2017/11/ICCT_Pocketbook_2017.pdf
- Kadijk, G., & Ligterink, N. (2012). *Road load determination of passenger cars*. (TNO Report: TNO, R10237). Retrieved from https://www.tno.nl/media/1971/road_load_determination_passenger_cars_tno_r10237.pdf
- Kadijk, G., Verbeek, M., Smokers, R., Spreen, J., Norris, J., Johnson, A., & Pagnac, J. (2012). *Supporting Analysis regarding Test Procedure Flexibilities and Technology Deployment for Review of the Light Duty Vehicle CO₂ Regulations*, 148. Retrieved from https://ec.europa.eu/clima/sites/clima/files/transport/vehicles/cars/docs/report_2012_en.pdf
- Kågeson, P. (1998). *Cycle-beating and the EU test cycle for cars*. European Federation for Transport and Environment (T&E): Brussels. Retrieved from http://www.transportenvironment.org/sites/te/files/media/T&E%2098-3_0.pdf
- Khalek, I. A., Bougher, T., & Jetter, J. J. (2010). Particle emissions from a 2009 gasoline direct injection engine using different commercially available fuels. *SAE International Journal of Fuels and Lubricants*, 3(2), 623–637. Retrieved from <https://doi.org/10.4271/2010-01-2117>
- Marotta, A., Pavlovic, J., Ciuffo, B., Serra, S., & Fontaras, G. (2015). Gaseous emissions from light-duty vehicles: Moving from NEDC to the new WLTP test procedure. *Environmental Science & Technology*, 49(14), 8315–8322. Retrieved from <https://doi.org/10.1021/acs.est.5b01364>
- Mellios, G., Hausberger, S., Keller, M., Samaras, Z., & Ntziachristos, L. (2011). *Parameterisation of fuel consumption and CO₂ emissions of passenger cars and light commercial vehicles for modelling purposes*. European Commission Joint Research Centre Technical Report EUR 24927 EN. Luxembourg: Publications Office of the European Union. Retrieved from http://publications.jrc.ec.europa.eu/repository/bitstream/11111111/22474/1/co2_report_jrc_format_final2.pdf
- Ministry of Environmental Protection of China. (2016a). *Limits and measurement methods for emissions from light-duty vehicles (China 6)*. Retrieved from http://www.mep.gov.cn/gkml/hbb/bgg/201612/t20161223_369497.htm
- Oberdörster, G., Sharp, Z., Atudorei, V., Elder, A., Gelein, R., Kreyling, W., & Cox, C. (2004). Translocation of inhaled ultrafine particles to the brain. *Inhalation toxicology*, 16(6-7), 437–445. Retrieved from <https://doi.org/10.1080/08958370490439597>
- Queiroz, C., & Tomanik, E. (1997). Gasoline direct injection engines - a bibliographical review. *SAE Technical Paper*, 973113. Retrieved from <https://doi.org/10.4271/973113>
- Storey, J. M., Lewis, S., Szybist, J., Thomas, J., Barone, T., Eibl, M., ... Kaul, B. (2014). Novel characterization of GDI engine exhaust for gasoline and mid-level gasoline-alcohol blends. *SAE International Journal of Fuels and Lubricants*, 7(2), 2014-01-1606. Retrieved from <https://doi.org/10.4271/2014-01-1606>
- Wang H., Hu J., Bao X., Wu Y., Xie S., & Li Z. (2010). Emission characteristics of gasoline taxi cabs complying with China IV emission standards during cold and hot starts. *Journal of Automotive Safety and Energy*, 1(2), 146–151. Retrieved from <http://www.journalase.com/EN/abstract/abstract8400.shtml>

- Weilenmann, M. F., Vasic, A. M., Stettler, P., & Novak, P. (2005). Influence of mobile air-conditioning on vehicle emissions and fuel consumption: A model approach for modern gasoline cars used in Europe. *Environmental Science and Technology*, 39(24), 9601-9610. Retrieved from <https://doi.org/10.1021/es050190j>
- Welstand, J. S., Haskew, H. H., Gunst, R. F., & Bevilacqua, O. M. (2003). Evaluation of the effects of air conditioning operation and associated environmental conditions on vehicle emissions and fuel economy. *SAE Technical Paper*, 2003-01-2247. Retrieved from <https://doi.org/10.4271/2003-01-2247>
- Weiss, M., Paffumi, E., Clairotte, M., Drossinos, Y., Vlachos, T., Bonnel, P., & Gieschaskiel, B. (2017). *Including cold-start emissions in the real-driving emissions (RDE) test procedure*. (JRC Science for Policy Report). Retrieved from <https://doi.org/10.2760/70237>
- Xiao, G., Yang, Z., & Isenstadt A. (2018). *Fuel efficiency technology trend assessment for LDVs in China – Advanced engine technology*. The International Council on Clean Transportation: Washington, DC. (In press)
- Yang, L. (2018) *Real-world emissions in China*. The International Council on Clean Transportation: Washington, DC. Retrieved from <https://www.theicct.org/publications/real-world-emissions-china-meta-study-pems-data>
- Zhang, S., & McMahon, W. (2012). Particulate emissions for LEV II light-duty gasoline direct injection vehicles. *SAE International Journal of Fuels and Lubricants*, 5(2), 2012-01-0442. Retrieved from <https://doi.org/10.4271/2012-01-0442>

APPENDIX

Table A1. LDV emission test equipment specifications

System	Model		Manufacturer	Range	Accuracy
Climatic Chamber	EC45192327		Imtech	Temp: -10 to 40°C	±1°C
				abs humidity: 5.5-12.2 g/kg	±5%RH
Dynamometer	RPL 1220		AVL	Speed: 0-200 km/h	±1%
				Force: 0-10,000 N	±1%
				Inertia(kg): 454-5400	±1%
Analyzer	CO	IRD i60	AVL	0-5000 ppm	±1%FS
	CO ₂	IRD i60	AVL	0-6.0%	±1%FS
	THC	FID i60	AVL	0-1000 ppmC3	±1%FS
	CH ₄	FID i60-cutter	AVL	0-3000 ppmC1	±1%FS
	NO _x	CLD i60	AVL	0-1000 ppm	±1%FS
PM system	PSS i60 LD		AVL	0-100 L/min	±2%
CVS system	CVS i60 LD		AVL	3-27 m ³ /min	±1%FS
PN counter	CPC3790		TSI	23 nm-3um 0-10,000 #/ccm	D50: 50±12% at 23nm D90: > 90% at 41nm ±10%
Filter Weight system	RX CH 500-03		AVL	Temp: 20-25°C	±1 °C
				Humidity: 40-50%	±3%RH
Scale	CPA2P-F		Sartorius	0/0.5/1.0/2.0 mg	±0.001 mg

Table A2. PEMS equipment specifications

	Principle	Range	Accuracy
CO	Heated NDIR	0-15 vol%	0-1499 ppm: ±30 ppm abs. 1500 ppm-49999 ppm: ±2% rel.
CO₂	Heated NDIR	0-20 vol%	0-9.99 vol%: ±0.1 vol% abs. 10-20 vol%: ±2% rel
NO	NDUV	0-5000 ppm	0-5000 ppm: ±0.2% FS or ±2% rel
NO₂	NDUV	0-2500 ppm	0-2500 ppm: ±0.2% FS or ±2% rel.
O₂	Sensor	0-25 vol%	±1 vol% of full scale at constant temperature and pressure
PN	Diffusion Charging	<0.2um 10 ⁴ to 2*10 ⁷ #/ccm	/
Exhaust flow	Pitot flow meter	18-810 kg/h (Flow rates at 100 °C)	±2.0% of reading or ±0.5% of full scale, whichever is greater